めに，IgG の高集積化および Fab 領域（抗原結合領域）の効果的な提示を実現し，抗体単体よりも高い抗原認識能と結合量を示し，余談ではあるが各種イムノアッセイ等の高感度化・高機能化にも貢献できた[18]。さて，ZZ-BNC には膜透過領域が残存しているので，薬剤等を封入したリポソームと効率的に複合体形成ができる。また，ZZ-BNC-リポソーム複合体が IgG を提示する時，ZZ-BNC が不必要な免疫反応を惹起する可能性がある Fc 領域を内部に固定するので，複合体全体の免疫原性の低減化も期待できる。

具体的な実例としては，EGF（epidermal growth factor）受容体を過剰発現しているグリオーマを脳内に移植したマウスに，抗 EGF 受容体抗体を提示した ZZ-BNC を脳内投与すると，グリオーマ特異的に ZZ-BNC が集積することが示されている[19]。また，ZZ-BNC を緑色蛍光タンパク質発現ベクターや 100 nm 蛍光ビーズを包含するリポソームと複合体化し，各種炎症部位に誘導されるセレクチン E（CD62E）に対する抗体を提示させ，網膜内にぶどう膜炎を誘導したマウスの尾静脈から投与したところ，網膜内の炎症部位特異的に緑色蛍光タンパク質の発現及び蛍光ビーズの送達が確認された。また，抗セレクチン E 抗体提示型 ZZ-BNC は，関節リュウマチのマウスモデルや心筋梗塞のラットモデルにおいて，静脈注射により速やかに各炎症部位へ移行することが判明している（鄭ら，投稿中）。以上から，ZZ-BNC 及び ZZ-BNC-リポソーム複合体は，試験管内のみならず生体内において遺伝子，抗癌剤，タンパク質など様々な物質を，提示する抗体の特異性依存的に標的細胞へ能動的に送達できることが示された。特に最近では，生体内で外来性抗原（ウイルスや細菌等）に対する免疫の中枢を担う樹状細胞を標的とするために，樹状細胞特異的に発現する細胞表層マーカー CD11c に対する抗体を提示した ZZ-BNC に，リポソームを介して日本脳炎ウイルスのワクチン抗原である D3 タンパク質を搭載してマウスに静脈内投与すると，D3 タンパク質単体の投与に比べて抗体が飛躍的に誘導されることを見出した（図 6）[20]。標的分子の CD11c は補体レセプターの一部であり，抗 CD11c 抗体は樹状細胞に強制的に抗原を認識させ，さらに抗原の取り込みが CD11c を介するエンドサイトーシスにより促進させたと考えられ，さらに ZZ-BNC が有する HBV 由来感染機構との相乗効果により，一層効果的な免疫誘導がもたらされたと考えている。現在，ナノ構造体に抗原を搭載して，樹状細胞による受動的な認識を期待するワクチンの創製が相次いでいるが，本抗 CD11c 抗体提示型 ZZ-BNC-リポソーム複合体によるワクチンは，能動的に樹状細胞を認識する「攻めのワクチン」であり，今後の様々な感染症疾患への応用が期待される。

次に，抗体以外の BNC の再標的化用分子とし

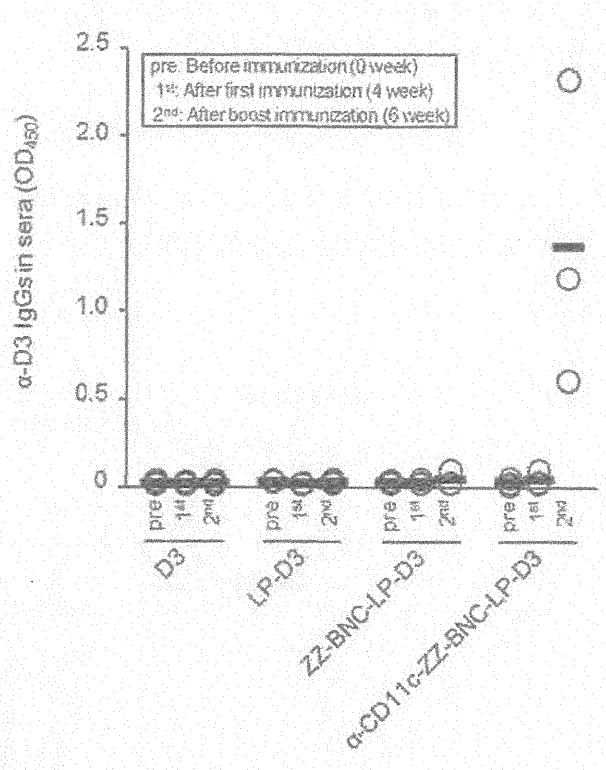

図 6　日本脳炎ウイルスワクチン抗原 D3 タンパク質を搭載した樹状細胞標的化バイオナノカプセル-リポソーム複合体を用いた抗原特異的 IgG 産生誘導

ては，リガンド，受容体，糖鎖，ホーミングペプチドなども検討されているが，特に顕著な効果を示したものはレクチンである。具体的には，糖鎖構造 β(1-6) GlcNAc は悪性度の高い腫瘍の表面に高頻度で見出され，糖転移酵素を導入することで同糖鎖構造を誘導した癌細胞は悪性度が増すことからも，β(1-6) GlcNAc を認識する能動的標的化 DDS 技術が開発されれば，診断及び癌治療において非常に有益である。一方，古くからβ(1-6) GlcNAc を認識するレクチン (PHA-L4) が特定の豆類に見出されていたが，PHA-L4 レクチン 1 分子では非常に親和性が弱く，β(1-6) GlcNAc を発現する細胞に選択的に薬剤等を送達する能力はなかった。筆者らは，ZZ-BNC 表層に多数存在するアミノ基に化学的にビオチン残基を導入し，ニュートラビジンを介して PHA-L4 レクチンを多数提示させ，ヒト大腸癌細胞 WiDr でβ(1-6) GlcNAc を発現する悪性度の高い腫瘍と，同細胞でβ(1-6) GlcNAc を発現しない腫瘍を背部皮下にそれぞれ有するヌードマウスに尾静脈から投与したところ，明らかに悪性度の高い腫瘍のみに BNC は集積することを見出した[21]。また，試験管内ながら PHA-L4 レクチンを提示する ZZ-BNC と緑色蛍光タンパク質発現ベクターを包含するリポソームの複合体は，β(1-6) GlcNAc を発現する細胞にのみ遺伝子導入していた[21]。以上から，BNC 及び BNC-リポソーム複合体は多彩な手法により再標的化可能な能動的標的化機構を有する DDS 用ナノキャリアであることが判明した。

4. おわりに

現在，実用化されている DDS 用ナノキャリアは，PEG 修飾やアルブミン修飾による長期血中滞留性に基づいた受動的薬剤送達を行うものが多い。また分子標的薬として，セツキシマブ (EGFR の機能を阻害する抗体で，癌細胞の増殖を抑制する) で代表されるような抗体医薬による抗癌剤が開発・販売されているが，それ自身が癌細胞の成長阻害薬として薬効を示すものが多く，様々な薬剤の送達に対応できるものではない。これらに対して本稿で紹介した BNC は，ウイルスの感染機構と安全性を兼ね備えたハイブリッドナノキャリアとして効果的な DDS を実現できる可能性を秘めている。再標的化用 BNC (ZZ-BNC) についても，抗体，タンパク質などの様々な標的親和性分子を介して，任意の標的化能を付与でき，様々な薬剤送達に対応できると考えられ，また抗体医薬シーズとの融合も期待される。現在，BNC に関する出願特許は 30 件以上にのぼり，そのうち約 20 件は，日本，韓国，米国，欧州において成立している。今後，BNC 技術を活用した新たな創薬研究の発展に期待したい。また，HBV 以外のウイルスの BNC 開発も可能であると考えられ，様々なウイルス由来の BNC が開発されることを期待している。

謝辞

本研究は，農研機構・生物系特定産業技術研究支援センター・イノベーション創出基礎的研究推進事業 (技術シーズ開発型・一般枠)，日本学術振興会科学研究費補助金 (基盤研究 A, 21240052)，厚生労働科学研究費補助金 (B 型肝炎創薬実用化等研究事業) の支援による成果であり，ここに謝意を表します。

参考文献

1) H. Maeda, J. Wu, T. Sawa, Y. Matsumura, and K. Hori, *J. Control Release*, **65**, 271-284 (2000).
2) S. J. Matthews and C. Mccoy, *Clin. Ther.*, **26**, 991-1025 (2004).
3) R. Kolhatkar, A. Lote, and H. Khambati, *Curr. Drug Discov.*, Technol., **8 (3)**, 197-206

(2011).
4) V. P. Torchilin, *Handb. Exp. Pharmacol.*, **197**, 3-53 (2010).
5) Y. Kaneda, *Adv. Drug Deliv. Rev.*, **64 (8)**, 730-738 (2012).
6) N. Subramanian, P. Mani, S. Roy, S. V. Gnanasundram, D. P. Sarkar, and S. Das, *J. Gen. Viol.*, **90 (8)**, 1812-1819 (2009).
7) S. Kuroda, S. Otaka, T. Miyazaki, M. Nakao, and Y. Fujisawa, *J Biol. Chem.*, **267**, 1953-1961 (1992).
8) J. Jung, M. Iijima, N. Yoshimoto, M. Sasaki, T. Niimi, K. Tatematsu, S. Y. Jeong, E. K. Choi, K. Tanizawa, and S. Kuroda, *Protein Expr. Purif.*, **78 (2)**, 149-155 (2011)
9) M. Yamada, A. Oeda, J. Jung, M. Iijima, N. Yoshimoto, T. Niimi, S. Y. Jeong, E. K. Choi, K. Tanizawa, and S. Kuroda, *J. Control Release*, **160 (2)**, 322-329 (2012).
10) I. Rodríguez-Crespo, E. Núñez, J. Gómez-Gutiérrez, B. Yélamos, J. P. Albar, D. L. Peterson, and F. Gavilanes, *J. Gen. Virol.*, **76**, 301-308 (1995).
11) S. Oess and E. Hildt, *Gene Ther.*, **7**, 750-758 (2000).
12) Y. Matsuura, H. Yagi, S. Matsuda, O. Itano, K. Aiura, S. Kuroda, M. Ueda, and Y. Kitagawa, *Eur. Surg. Res.*, **46**, 65-72 (2011).
13) T. Yamada, Y. Iwasaki, H. Tada, H. Iwabuki, M. K. Chuah, T. VandenDriessche, H. Fukuda, A. Kondo, M. Ueda, M. Seno, K. Tanizawa, and S. Kuroda, *Nat. Biotechnol.*, **21 (8)**, 885-890 (2003).
14) Y. Iwasaki, M. Ueda, T. Yamada, A. Kondo, M. Seno, K. Tanizawa, S. Kuroda, M. Sakamoto, and M. Kitajima, *Cancer Gene Ther.*, **14**, 74-81 (2007).
15) J. Jung, T. Matsuzaki, K. Tatematsu, T. Okajima, K. Tanizawa, and S. Kuroda, *J. Control Release*, **126 (3)**, 255-264 (2008).
16) T. Kasuya, J. Jung, R. Kinoshita, Y. Goh, T. Matsuzaki, M. Iijima, N. Yoshimoto, K. Tanizawa, and S. Kuroda, *Methods Enzymol.*, **464**, 147-166 (2009).
17) M. Iijima, H. Kadoya, S. Hatahira, S. Hiramatsu, G. Jung, A. Martin, J. Quinn, J. Jung,S. Y. Jeong, E. K. Choi, T. Arakawa, F. Hinako, M. Kusunoki, N. Yoshimoto, T. Niimi, K. Tanizawa, and S. Kuroda, *Biomaterials*, **32 (6)**, 1455-1464 (2011).
18) M. Iijima, T. Matsuzaki, N. Yoshimoto, T. Niimi, K. Tanizawa, and S. Kuroda, *Biomaterials*, **32 (34)**, 9011-9020 (2011).
19) Y. Tsutsui, K. Tomizawa, M. Nagita, H. Michiue, T. Nishiki, I. Ohmori, M. Seno, and H. Matsui, *J. Control Release*, **122 (2)**, 159-164 (2007).
20) H. Matsuo, N. Yoshimoto, M. Iijima, T. Niimi, J. Jung, S. Y. Jeong, E. K. Choi, T. Sewaki, T. Arakawa, and S. Kuroda, *Int. J. Nanomedicine*, **7**, 3341-3350 (2012).
21) T. Kasuya, J. Jung, H. Kadoya, T. Matsuzaki, K. Tatematsu, T. Okajima, E. Miyoshi, K. Tanizawa, S. Kuroda, *Hum. Gene Ther.*, **19 (9)**, 887-895 (2008).

解説

バイオナノカプセルを用いるイムノセンシング分子の整列化技術

Bio-nanocapsules for oriented immobilization of immunosensing molecules

キーワード
バイオナノカプセル
バイオセンシング
整列化
クラスター化
高機能化


飯嶋益巳　黒田俊一

バイオセンサーの機能（感度、特異性）を高めるためには、プローブ上のセンシング分子の整列化およびクラスター化が重要である。筆者らは、バイオナノカプセルによるセンシング分子整列化技術の開発に成功したので紹介する。

はじめに

生体分子間相互作用を特異的に検出するバイオアッセイおよびバイオセンサーは、医学、食品、環境、セキュリティー、生命科学研究等において非常に重要である。本稿では、最近筆者らが開発したセンシング分子の高機能化（高感度化、高特異性化）技術について、抗原抗体反応を例にとりながら、従来技術と比較しつつ概説する。

まず、固相上の抗原を検出する場合、ナノ粒子（金、銀、半導体、カーボンナノチューブ、シリカ、リポソーム等）の表層にIgGや標識物質を「クラスター化」させて感度上昇を図る方法が用いられている[1]。一方、液相中の抗原を検出する場合、固相上にIgGを「整列化」して固定し、抗原認識部位（Fv）周辺の立体障害を低減させて高感度化、高特異性化する方法が用いられている[2]。そこで、前述のナノ粒子を含む固相上にIgGを固定化するには、①IgGのリジン残基とN-ヒドロキシスクシンイミド基、②IgGのFc領域とProtein A/G、③IgG CH2領域の糖鎖還元末端とヒドラジン基、④IgGのC末端とカルボキシペプチダーゼY、⑤Fab'化抗体のシステイン残基とマレイミド基などの相互作用が用いられている。しかしながら、これらの方法は、固相とIgGをつなぐ足場分子自身の配向性を制御することが難しいため、IgG自身の整列化は不完全であった。また、化学修飾によるIgGの劣化も懸念され、「IgGの完全整列化」には、いまだ多くの課題が残されていた。

1. バイオナノカプセル（BNC）

BNCは、B型肝炎ウイルスの表面抗原Lタンパク質とリン脂質二重膜から形成される中空ナノ粒子で、出芽酵母内で自発的に平均直径約30 nmの粒子として高効率に生産可能である[3]。近年、筆者らはLタンパク質のN末端領域をProtein AのIgG-Fc結合Zドメイン（2量体）に置換したZZ-Lタンパク質からなるZZ-BNCを作製した（図1上）[4]。ZZ-BNCは、1粒子当たり最大60分子のIgGと自発的に結合することから、粒子表層でFv領域を放射状に整列化提示できると考えられた。そこで、筆者らは後述するように、ZZ-BNCが各種バイオアッセイやバイオセンサーにおいて、①IgGのクラスター化、②IgGの完全整列化、③固相上IgGの整列度合いの評価を実現するユニークなバイオマテリアルであることを見いだした（図1下）。

2. 液中ZZ-BNCによるIgGのクラスター化

ELISAにおいて、固相上の抗原（オボアルブミン、

筆者紹介：いいじま・ますみ（IIJIMA, Masumi）　名古屋大学大学院生命農学研究科（Grad. Sch. Bioagricultural Sci., Nagoya Univ.）研究員　1998年東京農業大学大学院農学研究科修士課程修了　博士（農学）　専門：ナノバイオテクノロジー
連絡先：〒464-8601 名古屋市千種区不老町　E-mail：iijimama@agr.nagoya-u.ac.jp（勤務先）
くろだ・しゅんいち（KURODA, Shun'ichi）　同上 教授　1986年京都大学大学院農学研究科修士課程修了　博士（農学）
専門：生物工学　連絡先：同上　E-mail：skuroda@agr.nagoya-u.ac.jp（勤務先）

OVA)に一次抗体を反応後、西洋ワサビペルオキシダーゼ(HRP)標識二次抗体をZZ-BNCとともに添加すると(図2A-2)、二次抗体のみの場合と比べて(図2A-1)、検出感度が著しく上昇した(約10倍)。また、アビジン-ビオチン複合体を併用すると、さらに感度は上昇した(約20倍)(図2A-3)[5]。一方、HRPより高分子のアルカリフォスファターゼ(ALP)で標識した二次抗体の場合、立体障害によりZZ-BNCの増感効果は観察されなかったが、IgG-ALP間リンカー長の最適化により回避できることを見いだした[6]。次に、蛍光イムノアッセイにおいて、固相上の抗原に、一次抗体と蛍光色素標識ZZ-BNCを混合して添加すると、通常の蛍光標識二次抗体の場合と比べて、検出感度が著しく上昇した(約10倍)[7]。以上から、ZZ-BNCは検出用抗体を表層にクラスター化および整列化し、検出用抗体1分子当たりの標識酵素および蛍光色素の分子数を高めると考えられた。

さらに、同一試料に含まれる様々な抗原の局在、存在量を同時に検出する場合、通常は一次抗体の動物種またはサブクラスの重複を避けて、それぞれに対応する二次抗体を使用するので、各種抗体の利用可能性が律速となり同時検出を断念することも多かった。そこで、ZZ-BNCを様々な蛍光色素(Cy2、Cy3、Cy5、Cy7)で標識し、4種類の抗原に対する抗体(3種類はマウスIgG2a)をそれぞれ提示させ、4種類の抗原を含むブロットに使用したところ、各抗原を高感度かつ同時に検出することができた(図2B)[7]。以上の結果は、ZZ-BNCは、免疫化学的検出において長年技術的課題であった使用抗体の動物種およびサブクラスに関する

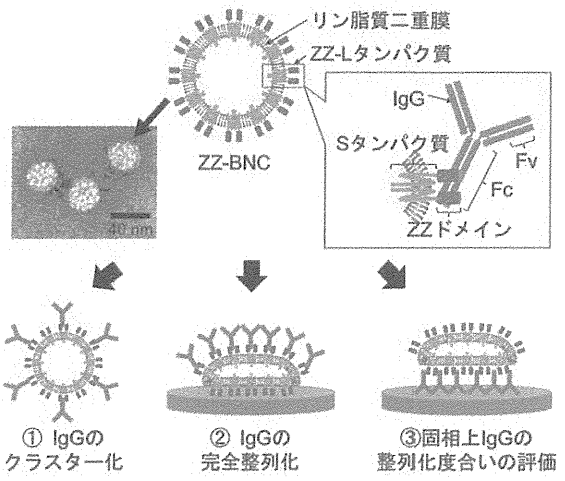

図1 ZZ-BNCの構造と機能

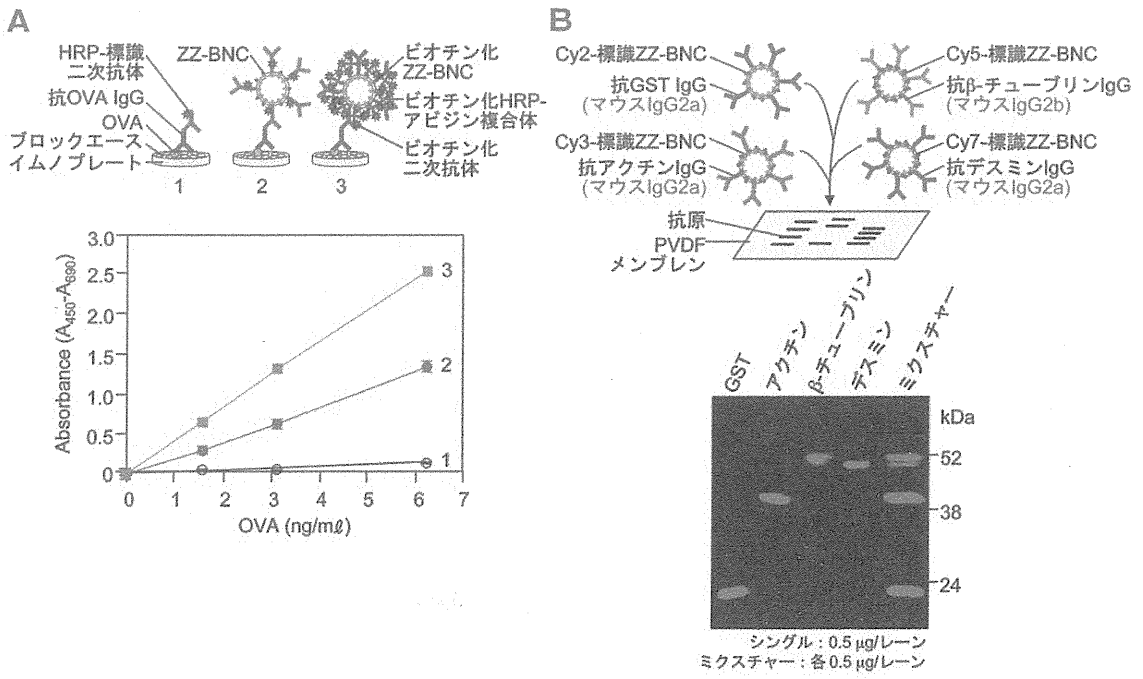

図2 ZZ-BNCによるELISAの高感度化(A)および蛍光免疫法における複数抗原の同時検出(B)
(右下写真 文献[7]より転載)

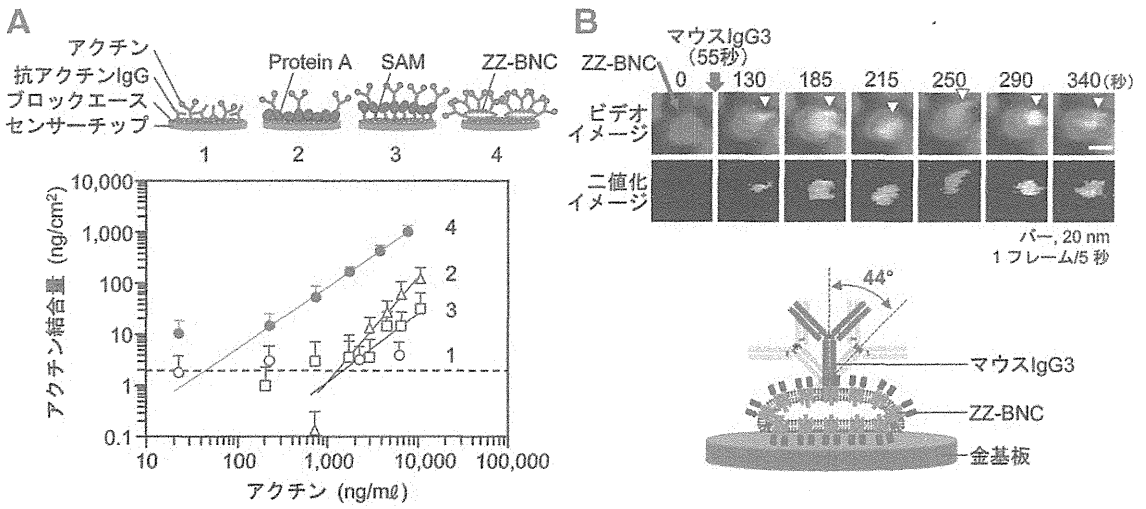

図 3　ZZ-BNC による QCM バイオセンサーの高感度化 (A) および HS-AFM を用いた ZZ-BNC と IgG の結合のビデオ観察 (B)
(右上写真 文献[9] より一部転載)

制限を根本的に解消できることを示している。

3. 固定化 ZZ-BNC による IgG の整列化

水晶発振子微量天秤 (QCM) および表面プラズモン共鳴 (SPR) におけるイムノセンサー (主に金基板) では、従来、IgG は「直接固定」、「Protein A を介して固定」、および「自己組織化単分子膜 (SAM) 修飾 Protein A を介して固定」されるが[2]、筆者らは、ZZ-BNC を介して IgG を固定した金基板を検討したところ、単位抗体量当たりの抗原結合量、検出感度、抗原への親和性のいずれもが著しく上昇していることを見いだした (図 3A)[8]。これは、IgG の Fc 領域が ZZ-BNC 表層に固定され、Fv 領域が放射状に整列化し、IgG-Fv 領域周辺の立体障害が著しく改善されたためと考えられた。また、QCM センサーにおける ZZ-BNC の抗体結合能は、酸処理による抗体の脱着を 20 回以上繰り返しても変わらないほど耐久性が高いことも判明した。

そこで、生体分子の溶液中の挙動をリアルタイムに観察できる高速原子間力顕微鏡 (HS-AFM) を用いて、ZZ-BNC と IgG の溶液中での状態を解析した。まず、ZZ-BNC の表面積から溶液中の ZZ-BNC の直径は約 40 nm と算出され、ZZ-L タンパク質の 2 量体が直径約 6 nm の突起として約 54 個存在することが判明した[9]。また、溶液中のマウス IgG3 はヒンジ部分で折り曲がった状態と Y 字型の伸びた状態で存在していた。次に、固定化 ZZ-BNC と IgG の結合様式を HS-AFM でビデオ観察したところ、これまでに予想された通り、IgG 分子が ZZ-BNC 上で Fc 領域を支点として回転ブラウン運動を行っていることが判明した (平均速度 0.92 nm/秒、最大角度 44°) (図 3B)。以上から、ZZ-BNC は抗体のナノレベル整列化およびクラスター化の足場として有効であることが証明された。また、この観察例はバイオセンサー表面センシング分子を世界で初めてリアルタイム観察したものであり、今後のセンサー開発において HS-AFM がセンシング分子のナノレベル配向性評価に有効であることを示している。

4. 液中 ZZ-BNC による固相上の IgG の整列化度合いの評価

イムノセンサーにおいて固定化 IgG の配向性を最適化することは非常に重要である。通常は、抗原結合量により同配向性を最適化するが、間接的な方法であり、本当に固定化 IgG の整列化が達成されているかは不明である。最近では、AFM、電子顕微鏡、飛行時間二次イオン質量分析計、前項の HS-AFM などの大型分析機械を用いて、基板表面の形状や固定化抗体の配向性に依存した遊離アミノ酸などに基づき評価されている[2]。しかし、イムノセンサーは幅広い領域で用いられているので、簡便かつ直接的に固定化 IgG の配向性を評価する方法が必要である。そのような中、筆者らは液中抗原を検出するサンドイッチイムノアッセイにおける ZZ-BNC の増感効果を最適化する過程

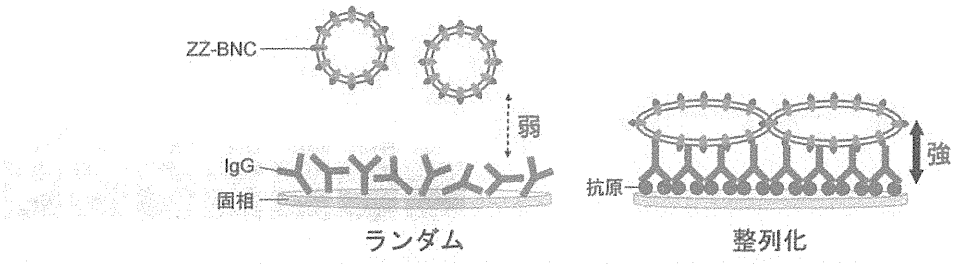

図4 液中ZZ-BNCによる固相上のIgGの整列化度合いの評価

で、図4に示すように、基板上にランダムに固定化されたIgGよりも、抗原依存的に整列固定化されたIgGに対し、ZZ-BNCが単独で高い親和性を示すことを見いだした[10]。これは、ZZ-BNCが、固相上IgGの配向性を評価するプローブとして有効であることを示している。

さらに、サンドイッチイムノアッセイでは、二次抗体が検出用IgG(液相中)のみを認識する必要があるため、通常、検出用IgGと異なる動物種やサブクラスの捕捉用IgG(固相上)を使用する。そこで、二次抗体の代わりにZZ-BNCを用いて、同一抗体による抗原のサンドイッチイムノアッセイを行ったところ、ZZ-BNCは固相上の「捕捉用IgG−抗原−検出用IgG」複合体のみと特異的に結合した[10]。これは、捕捉用IgGに結合した抗原により整列化した検出用IgGにZZ-BNCが特異的に結合したためである。以上の結果は、サンドイッチイムノアッセイにおいて長年の技術的課題であった使用抗体に関する制限を、ZZ-BNCが解消できたことを示している。

おわりに

本稿では、最も身近な生体分子間相互作用である抗原抗体反応に注目して、ZZ-BNCのユニークな3つの機能(IgGクラスター化、IgG整列化、固定化IgGの整列化度合いの評価)について述べてきた。しかしながら、生命現象を支える生体分子間相互作用は、抗原と抗体以外にも、リガンドとレセプター、レクチンと糖鎖、DNAと核酸結合タンパク質など多く存在する。今後は、ZZ-BNCの足場分子としての高い安定性を活用して、抗体分子以外の前述センシング分子をナノレベル整列化技術に応用し、幅広いバイオアッセイおよびバイオセンサーの高感度化、高特異性化を行いたい。

最後に、本研究遂行に当たり、ご援助をいただいた、日本学術振興会科学研究費補助金・基盤研究(A)(21240052、25242043(黒田))、若手研究(B)(23710143、25870310(飯嶋))、㈱農業・食品産業技術総合研究機構・生物系特定産業技術研究支援センター(黒田)、厚生労働科学研究費補助金(黒田)に深謝致します。

参考文献

1) Liu, G. *et al.*: Nanomaterial labels in electrochemical immunosensors and immunoassays, *Talanta*, 74, 308 ～ 317 (2007)
2) Trilling, A. K. *et al.*: Antibody orientation on biosensor surfaces: a minireview, *Analyst*, 138, 1619 ～ 1627 (2013)
3) Jung, J. *et al.*: Efficient and rapid purification of drug-and gene-carrying bio-nanocapsules, hepatitis B virus surface antigen L particles, from *Saccharomyces cerevisiae*, *Protein Exp. Purif.*, 78, 149 ～ 155 (2011)
4) Kasuya, T. *et al.*: Chapter 8-Bio-nanocapsule-liposome conjugates for *in vivo* pinpoint drug and gene delivery, *Methods Enzymol.*, 464, 147 ～ 166 (2009)
5) Iijima, M. *et al.*: Bionanocapsule-based enzyme-antibody conjugates for enzyme-linked immunosorbent assay, *Anal. Biochem.*, 396, 257 ～ 261 (2010)
6) Iijima, M. *et al.*: Bio-nanocapsules for signal enhancement of alkaline phosphatase-linked immunosorbent assays, *Biosci. Biotechnol. Biochem.*, 77, 120760-1 ～ 120760-4 (2013)
7) Iijima, M. *et al.*: Fluorophore-labeled nanocapsules displaying IgG Fc-binding domains for the simultaneous detection of multiple antigens, *Biomaterials*, 32, 9011 ～ 9020 (2011)
8) Iijima, M. *et al.*: Nanocapsules incorporating IgG Fc-binding domain derived from *Staphylococcus aureus* protein A for displaying IgGs on immunosensor chips, *ibid.*, 32, 1455 ～ 1464 (2011)
9) Iijima, M. *et al.*: Nano-visualization of oriented-immobilized IgGs on immunosensors by high-speed atomic force microscopy, *Sci. Rep.*, 2, 790, DOI: 10.1038/srep 00790, (2012)
10) Iijima, M. *et al.*: Nanocapsule-based probe for evaluating the orientation of antibodies immobilized on a solid phase, *Analyst*, 138, 3470 ～ 3477 (2013)

Genes & Development

Targeting of MCL-1 kills MYC-driven mouse and human lymphomas even when they bear mutations in *p53*

Gemma L. Kelly, Stephanie Grabow, Stefan P. Glaser, et al.

Genes Dev. 2014 28: 58-70
Access the most recent version at doi:10.1101/gad.232009.113

Targeting of MCL-1 kills MYC-driven mouse and human lymphomas even when they bear mutations in *p53*

Gemma L. Kelly,[1,2,3,7] Stephanie Grabow,[1,3] Stefan P. Glaser,[1,3] Leah Fitzsimmons,[2] Brandon J. Aubrey,[1,3] Toru Okamoto,[1,3,6] Liz J. Valente,[1,3] Mikara Robati,[1] Lin Tai,[1] W. Douglas Fairlie,[1,3] Erinna F. Lee,[1,3] Mikael S. Lindstrom,[4] Klas G. Wiman,[4] David C.S. Huang,[1,3] Philippe Bouillet,[1,3] Martin Rowe,[2] Alan B. Rickinson,[2] Marco J. Herold,[1,3,5] and Andreas Strasser[1,3,5,7]

[1]The Walter and Eliza Hall Institute, Parkville, Victoria 3052, Australia; [2]School of Cancer Sciences, University of Birmingham College of Medical and Dental Sciences, The University of Birmingham, Edgbaston, Birmingham B15 2TT, United Kingdom; [3]Department of Medical Biology, The University of Melbourne, Parkville, Victoria 3050 Australia; [4]Department of Oncology–Pathology, Karolinska Institute, Cancer Center Karolinska (CCK), SE-171 76 Stockholm, Sweden

The transcriptional regulator c-MYC is abnormally overexpressed in many human cancers. Evasion from apoptosis is critical for cancer development, particularly c-MYC-driven cancers. We explored which anti-apoptotic BCL-2 family member (expressed under endogenous regulation) is essential to sustain c-MYC-driven lymphoma growth to reveal which should be targeted for cancer therapy. Remarkably, inducible Cre-mediated deletion of even a single *Mcl-1* allele substantially impaired the growth of c-MYC-driven mouse lymphomas. Mutations in *p53* could diminish but not obviate the dependency of c-MYC-driven mouse lymphomas on MCL-1. Importantly, targeting of MCL-1 killed c-MYC-driven human Burkitt lymphoma cells, even those bearing mutations in *p53*. Given that loss of one allele of *Mcl-1* is well tolerated in healthy tissues, our results suggest that therapeutic targeting of MCL-1 would be an attractive therapeutic strategy for MYC-driven cancers.

[*Keywords*: cancer; apoptosis; MCL-1; p53; BCL-2; MYC]

Supplemental material is available for this article.

Received October 1, 2013; revised version accepted November 19, 2013.

The c-MYC transcription factor regulates ~10,000 genes, including many that control cell growth and division (Dang 1999). Deregulated c-MYC expression is detected in up to 70% of human cancers, including lymphomas and leukemias (Boxer and Dang 2001; Sanchez-Beato et al. 2003). Much of what we know about c-MYC-driven tumorigenesis has emerged from studies using *Eμ-Myc* transgenic mice, in which the *c-Myc* transgene is subjugated to the immunoglobulin (*Ig*) heavy chain gene enhancer (*Eμ*), mimicking the consequences of the *c-MYC/IGH* or *c-MYC/IGL* chromosomal translocations that drive human Burkitt lymphoma (Adams et al. 1985). The *Eμ-Myc* mice exhibit a preleukemic expansion of pre-B cells that precedes the outgrowth of clonal sIg^- pre-B-cell or sIg^+ B-cell lymphomas arising with a median latency of ~110 d (Adams et al. 1985; Langdon et al. 1986).

Evasion from cell death is a hallmark of cancer, particularly those driven by c-MYC (Hanahan and Weinberg 2011; Kelly and Strasser 2011). Deregulated c-MYC expression enhances cell death under unfavorable growth conditions, such as limited availability of growth factors, through the intrinsic apoptotic pathway that is regulated by interactions of proteins belonging to three functionally distinct subgroups of the BCL-2 family (Youle and Strasser 2008). Following apoptotic stimuli, the proapoptotic BH3-only proteins (e.g., BIM and PUMA) become transcriptionally and/or post-transcriptionally up-regulated. For example, in response to DNA damage or oncogenic stress, the tumor suppressor p53 directly transcriptionally activates PUMA and NOXA to cause cell death (Jeffers et al. 2003; Villunger et al. 2003). The BH3-only proteins directly or indirectly activate BAX/BAK, the executioners of apoptosis, which permeabilize the outer

[5]**These authors contributed equally to this work.**
[6]**Present address: Department of Molecular Virology, Research Institute for Microbial Diseases, Osaka University, Osaka, Japan.**
[7]**Corresponding authors**
E-mail strasser@wehi.edu.au
E-mail gkelly@wehi.edu.au
Article is online at http://www.genesdev.org/cgi/doi/10.1101/gad.232009.113.

mitochondrial membrane and thereby unleash the downstream caspase cascade for cellular demolition (Merino et al. 2009; Llambi et al. 2011).

Apoptotic blocks, such as overexpression of prosurvival BCL-2-like proteins (Strasser et al. 1990; Swanson et al. 2004) or loss of proapoptotic BIM or PUMA (Egle et al. 2004; Hemann et al. 2004; Michalak et al. 2009), accelerate c-MYC-driven lymphomagenesis. Interestingly, mutations that deregulate the intrinsic apoptotic pathway, including amplifications of the genomic regions encoding *MCL-1* and *BCL-X* (Beroukhim et al. 2010), are detected in human tumors and are often associated with poor chemotherapy responses (Khaw et al. 2011). Burkitt lymphoma is associated with frequent loss of BIM and/or PUMA expression, in part due to gene hypermethylation (Mestre-Escorihuela et al. 2007; Garrison et al. 2008; Richter-Larrea et al. 2010; Giulino-Roth et al. 2012). Moreover, many Burkitt lymphomas contain defects in the p53 tumor suppressor pathway, particularly mutations in *p53* itself (Farrell et al. 1991; Bhatia et al. 1992) but also overexpression of the ubiquitin ligase HDM2 (called MDM2 in mice) or loss of the p14/ARF locus (Lindstrom et al. 2001).

Although overexpression of prosurvival BCL-2 family members accelerates c-MYC-induced lymphomagenesis, it is unclear whether the sustained survival and growth of c-MYC-driven lymphomas depends on the expression of these proteins under endogenous regulation. This remains an important question because knowledge of which prosurvival protein is essential for the sustained growth of a particular cancer will pinpoint the family member that should be targeted by the emerging BH3 mimetic drugs (Lessene et al. 2008). Using innovative gene targeting and drug-mimicking tools, we show for the first time that MCL-1 targeting kills c-MYC-driven mouse and human lymphoma cells even when p53 is mutated. This is remarkable given that we found that p53 does affect the dependency of these lymphoma cells on MCL-1 and suggest that therapeutic targeting of MCL-1 may be a promising strategy for cancer therapy.

Results

Experimental strategy to determine which anti-apoptotic BCL-2 family member is essential for the sustained survival and expansion of MYC-driven lymphomas

To examine the roles of BCL-X_L and MCL-1 expression under endogenous control in the sustained growth of *Eμ-Myc* lymphomas, we generated mice in which we could genetically delete *Mcl-1* or *Bcl-x* at will exclusively within c-MYC-driven lymphoma cells. Specifically, we produced *Eμ-Myc* transgenic mice that express a tamoxifen-regulated Cre recombinase-estrogen receptor fusion protein from the ubiquitously expressed Rosa26 locus (Rosa26-CreERT2 mice) (Seibler et al. 2003) and bear *loxP* targeted (*floxed*, denoted *fl*) alleles of the prosurvival gene *Bcl-x* (Wagner et al. 2000) or *Mcl-1* (Vikstrom et al. 2010) (Supplemental Fig. 1). As expected, the progeny with all three genetic alterations developed lymphomas with the same latency as standard *Eμ-Myc* mice (Supplemental Fig. 2A) because they expressed normal levels of BCL-X_L or MCL-1. The lymphoma cells were transplanted into C57BL/6-Ly5.1$^+$ recipients, which were treated with tamoxifen to activate the Cre-ERT2 recombinase, leading to deletion of *Bcl-x^{fl}* or *Mcl-1^{fl}* alleles exclusively within the malignant cells (Supplemental Fig. 1). Selected primary lymphomas were infected with an Ub-GFP-Luciferase lentivirus to facilitate monitoring lymphoma progression/regression following *Bcl-x* or *Mcl-1* deletion by imaging for bioluminescence in C57BL/6-albino recipient mice (Supplemental Fig. 1). In mice transplanted with *Eμ-Myc;CreERT2* lymphoma cells lacking any floxed allele (for simplicity, hereafter termed "control"), tumor expansion did not differ significantly between untreated and tamoxifen-treated recipients ($P = 0.06$) (Supplemental Fig. 2B). This shows that CreERT2 activation per se does not impair the growth of *Eμ-Myc* lymphomas.

Homozygous loss of Bcl-x only slightly impairs the sustained growth of Eμ-Myc lymphomas

Since endogenous BCL-X_L is necessary for *Eμ-Myc*-induced lymphoma development (Kelly et al. 2011), we predicted that it might also be essential for the sustained expansion of such malignant lymphomas. To examine this, primary lymphomas from nine *Eμ-Myc;CreERT2;Bcl-x$^{fl/fl}$* and seven control mice were transplanted into C57BL/6-Ly5.1$^+$ recipient mice and cohorts treated with tamoxifen. Homozygous *Bcl-x* loss resulted in only a modest delay in tumor expansion and slightly prolonged survival of the mice (median survival 25 d for *Eμ-Myc;CreERT2;Bcl-x$^{fl/fl}$* vs. 19 d for the controls; [*] $P = 0.0367$) (Fig. 1A). Following homozygous *Bcl-x* deletion, only 4% of the recipient mice (three from 73) showed complete lymphoma regression, which is comparable with the 3% of the tamoxifen-treated mice (one from 32) bearing control tumors.

This result was confirmed by in vivo lymphoma bioluminescence imaging (Fig. 1B). As early as 7 d after tumor transplant, the recipients displayed a significant lymphoma burden ($\geq 1 \times 10^7$ photon flux per second). These lymphomas continued to grow following tamoxifen treatment to delete both *Bcl-x* alleles and overwhelmed the recipients only shortly after the untreated mice had succumbed to the same lymphomas that retained *Bcl-x*. Efficient deletion of the *Bcl-x* alleles and loss of the BCL-X_L protein were confirmed by quantitative RT–PCR (qRT–PCR) and Western blot analyses in paired tamoxifen-treated and untreated lymphomas taken from mice transplanted with *Eμ-Myc;CreERT2;Bcl-x$^{fl/fl}$* lymphomas (Supplemental Fig. 3). These data reveal that malignant *Eμ-Myc* lymphomas can continue to grow without endogenous BCL-X_L expression.

Loss of Mcl-1 substantially impairs the sustained growth of Eμ-Myc lymphomas

In parallel experiments, we investigated whether MCL-1 was essential for the sustained growth of *Eμ-Myc* lymphomas. Cohorts of C57BL/6-Ly5.1$^+$ mice were transplanted with independent primary lymphomas from six

Eμ-Myc;CreERT2;Mcl-1$^{fl/fl}$ and seven control mice, and their survival was compared following tamoxifen treatment (Fig. 2). Strikingly, in 30% of the recipients, homozygous deletion of *Mcl-1* provoked complete lymphoma regression and extended survival (>180 d post-transplant) (Fig. 2A). The dramatic tumor regression was confirmed by bioluminescence imaging of lymphomas transplanted into C57BL/6-albino recipient mice (Fig. 2B). Importantly, even the tamoxifen-treated recipients that relapsed exhibited substantially extended survival compared with those bearing control lymphomas (median survival 35 d for mice bearing *Eμ-Myc;CreERT2;Mcl-1$^{fl/fl}$* lymphomas vs. 19 d for those bearing control lymphomas; [****] $P < 0.0001$).

Remarkably, even heterozygous *Mcl-1^{fl}* loss substantially impaired sustained lymphoma growth: 20% of recipient mice bearing *Eμ-Myc;CreERT2;Mcl-1$^{fl/+}$* lymphomas showed prolonged survival after tamoxifen treatment (median survival was 23 d for relapsing lymphomas vs. 19 d for control mice; [****] $P < 0.0001$) (Fig. 2A). These results demonstrate that the level of MCL-1 is highly critical for the sustained survival and expansion of MYC-driven lymphomas. This conclusion was strengthened by further analysis of the relapsing tamoxifen-treated lymphomas. The conditional allele of *Mcl-1* carries a human (hu) *CD4* reporter gene, which is expressed following *Mcl-1^{fl}* recombination, thus permitting single-cell analysis of the recombination efficiency (Vikstrom et al. 2010; Glaser et al. 2012). Strikingly, ~60% of *Eμ-Myc;CreERT2;Mcl-1$^{fl/+}$* and 40% of *Eμ-Myc;CreERT2;Mcl-1$^{fl/fl}$* lymphomas that relapsed following tamoxifen treatment had escaped deletion of their conditional *Mcl-1* alleles mostly because they had undergone selection for loss of CreERT2 expression (Fig. 3A,B). Western blot analysis of these tamoxifen-treated tumors confirmed that MCL-1 protein expression was not reduced (Fig. 3B). In addition, the minority of *Eμ-Myc;CreERT2;Mcl-1$^{fl/fl}$* lymphomas that did relapse as huCD4-positive following tamoxifen treatment had only recombined one allele of *Mcl-1* and continued to express MCL-1 protein (Fig. 3C,D). By inference, the survival curves described earlier grossly underestimate the role that MCL-1 plays in the sustained growth of *Eμ-Myc* lymphomas. Indeed when animals that succumbed to relapsed lymphomas that had selected

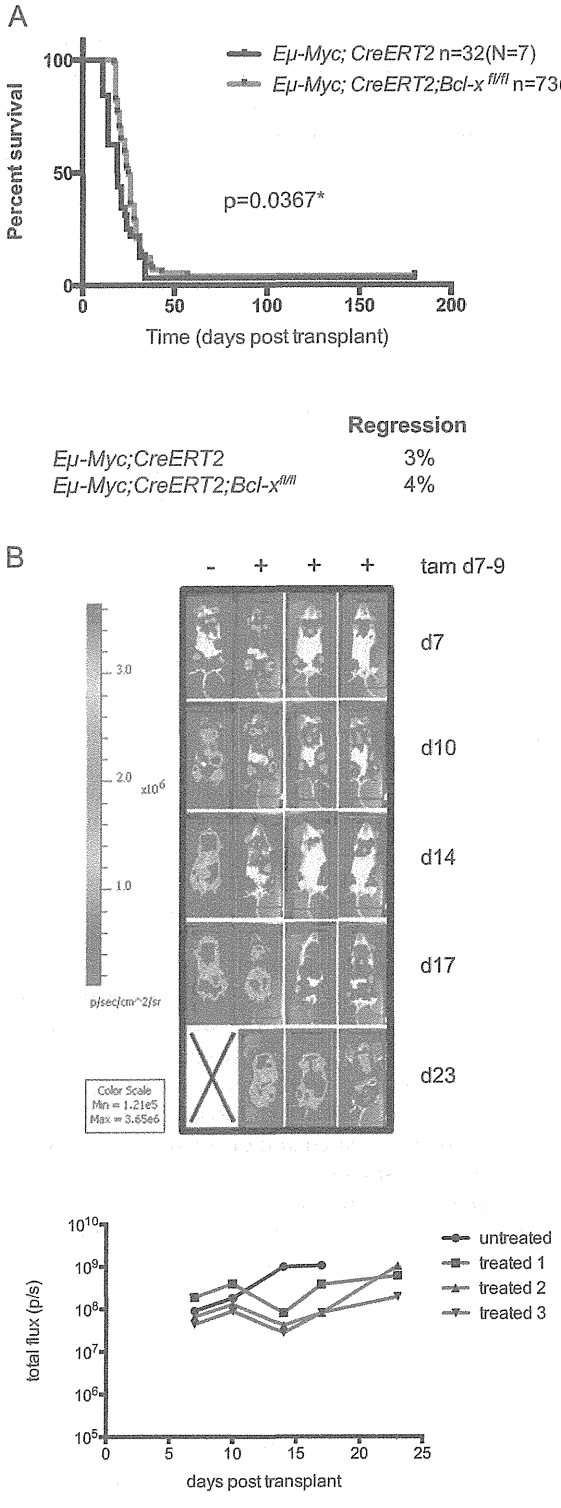

Figure 1. Homozygous loss of *Bcl-x* has only a minor impact on the growth of *Eμ-Myc* lymphomas. (*A*) Survival curves of C57BL/6-Ly5.1$^+$ recipient mice transplanted with *Eμ-Myc;CreERT2;Bcl-x$^{fl/fl}$* (green line) or control (*Eμ-Myc;CreERT2*; black line) lymphoma cells and treated with tamoxifen to inactivate *Bcl-x* where applicable. (n) Total number of recipient mice analyzed; (N) number of independent lymphomas tested. Homozygous deletion of *Bcl-x* resulted in a small but significant delay in tumor growth. (*) $P = 0.0367$. For the mice transplanted with the control *Eμ-Myc;CreERT2* lymphomas, 3% regressed, and the overall median survival was 19 d. For the mice transplanted with the *Eμ-Myc;CreERT2;Bcl-x$^{fl/fl}$* lymphomas, 4% regressed, and the overall median survival was 25 d. (*B*) Bioluminescence imaging of the tumor burden in C57BL/6-albino recipient mice injected with primary *Eμ-Myc;CreERT2;Bcl-x$^{fl/fl}$* lymphoma cells that had been transduced with a lentiviral vector coexpressing GFP and luciferase. At 7 d post-transplant, a cohort of these mice was treated with tamoxifen. Mice were subsequently imaged for bioluminescence to monitor lymphoma burden every 3–4 d by measuring the total photon flux per second emitted from a region of interest (ROI) drawn around the whole mouse. See also Supplemental Figure 3.

against loss of *Mcl-1*^{fl} alleles were removed from the analysis (and those lymphomas that had mutated *p53* alleles were also removed from the survival curves) (Fig. 5A; see below), nearly 100% of animals survived lymphoma-free long-term (>180 d post-transplant) (Fig. 3E). These findings reveal that even heterozygous *Mcl-1* loss is highly detrimental for the sustained in vivo growth of malignant *Eμ-Myc* lymphomas, indicating that relatively weak targeting of MCL-1 might have therapeutic benefits in MYC-driven cancers.

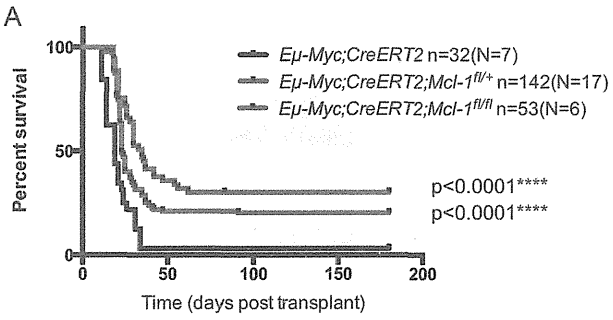

	Regression
Eμ-Myc;CreERT2	3%
Eμ-Myc;CreERT2;Mcl-1$^{fl/+}$	20%
Eμ-Myc;CreERT2;Mcl-1$^{fl/fl}$	30%

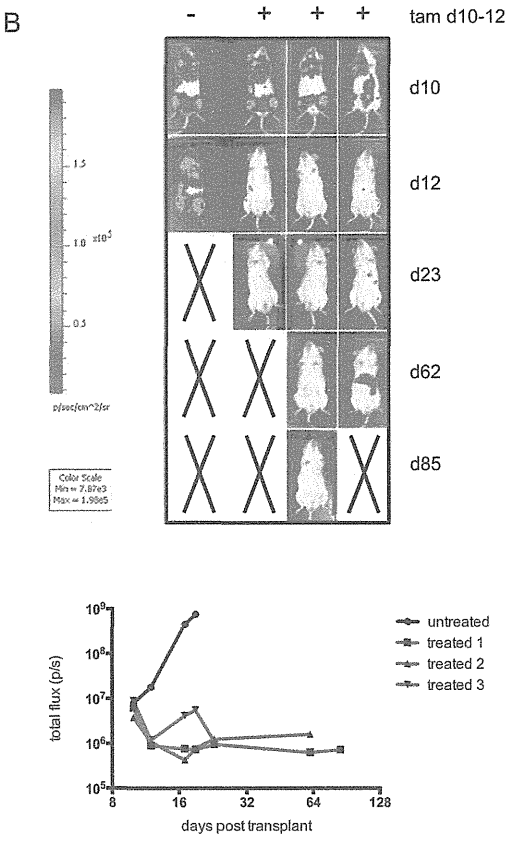

The sustained growth of human Burkitt lymphoma cells depends on the expression of MCL-1

We sought to translate these findings into the human disease setting. Western blot analysis of Burkitt lymphoma cell lines revealed that all expressed MCL-1 with heterogeneous expression of BCL-X_L and, as previously reported (Henderson et al. 1991) little to no BCL-2 (Fig. 4A). As a control for the BCL-2 antibody, we showed that the X50-7 and Awia-tr lymphoblastoid cell lines expressed high levels of this prosurvival protein (Fig. 4A), as reported (Henderson et al. 1991).

To examine the impact of targeting BCL-2 prosurvival proteins on Burkitt lymphoma growth, we developed a novel assay based on doxycycline (dox)-inducible expression (from a lentiviral vector) of genetically engineered variants of the BH3-only protein BIM_S with select binding specificities for distinct BCL-2 prosurvival proteins (Fig. 4B; Chen et al. 2005; Lee et al. 2008). These polypeptides have a mechanism of action similar to that of BH3 mimetic drugs; i.e., they antagonize BCL-2 prosurvival protein function by engaging a hydrophobic ligand-binding groove on their surface (Lee et al. 2007, 2008; Souers et al. 2013). The wild-type BIM_S, which binds with high affinity to all BCL-2 prosurvival proteins, served as a positive control for the integrity of the intrinsic apoptotic pathway. Mutant BIM_S4E, which does not bind to any BCL-2 prosurvival family member, thus served as a negative control. L62A/F69A mutant BIM_S2A preferentially binds MCL-1, and BIM_SBAD binds to BCL-2, BCL-X_L, and BCL-W. Western blotting verified inducible expression of all BIM_S variants in Rael-BL (Fig. 4C) and other Burkitt lymphoma cell lines (Supplemental Fig. 4A). All Burkitt lymphoma cell lines tested were highly sensitive to the expression of wild-type BIM_S, demonstrating that they had an intact intrinsic apoptotic pathway. Conversely, as expected, these cells were not affected by BIM_S4E (representative FACS plots are shown in Supplemental Fig. 4B).

Figure 2. Loss of *Mcl-1*, even loss of a single allele, greatly impairs the sustained growth of *Eμ-Myc* lymphomas within the whole animal. (*A*) Survival curves of C57BL/6-Ly5.1$^+$ recipient mice transplanted with *Eμ-Myc;CreERT2;Mcl-1*$^{fl/+}$ (red line), *Eμ-Myc;CreERT2;Mcl-1*$^{fl/fl}$ (blue line), or control (*Eμ-Myc;CreERT2*; black line) lymphoma cells and treated with tamoxifen to inactivate *Mcl-1* where applicable. (n) Total number of recipient mice analyzed; (N) number of independent lymphomas tested. Heterozygous and homozygous deletion of *Mcl-1* significantly delayed lymphoma growth. (****) $P < 0.0001$. For the mice transplanted with the control *Eμ-Myc;CreERT2* lymphomas, 3% regressed, and the overall median survival was 19 d. For the mice transplanted with the *Eμ-Myc;CreERT2;Mcl-1*$^{fl/+}$ lymphomas, 20% regressed, and the overall median survival was 23 d. For the mice transplanted with the *Eμ-Myc;CreERT2;Mcl-1*$^{fl/fl}$ lymphomas, 30% regressed, and the overall median survival was 35 d. (*B*) Bioluminescence imaging of the tumor burden in C57BL/6-albino recipient mice injected with primary *Eμ-Myc;CreERT2;Mcl-1*$^{fl/fl}$ lymphoma cells. At 10 d post-transplant, a cohort of these mice was treated with tamoxifen. These mice were subsequently imaged for bioluminescence.

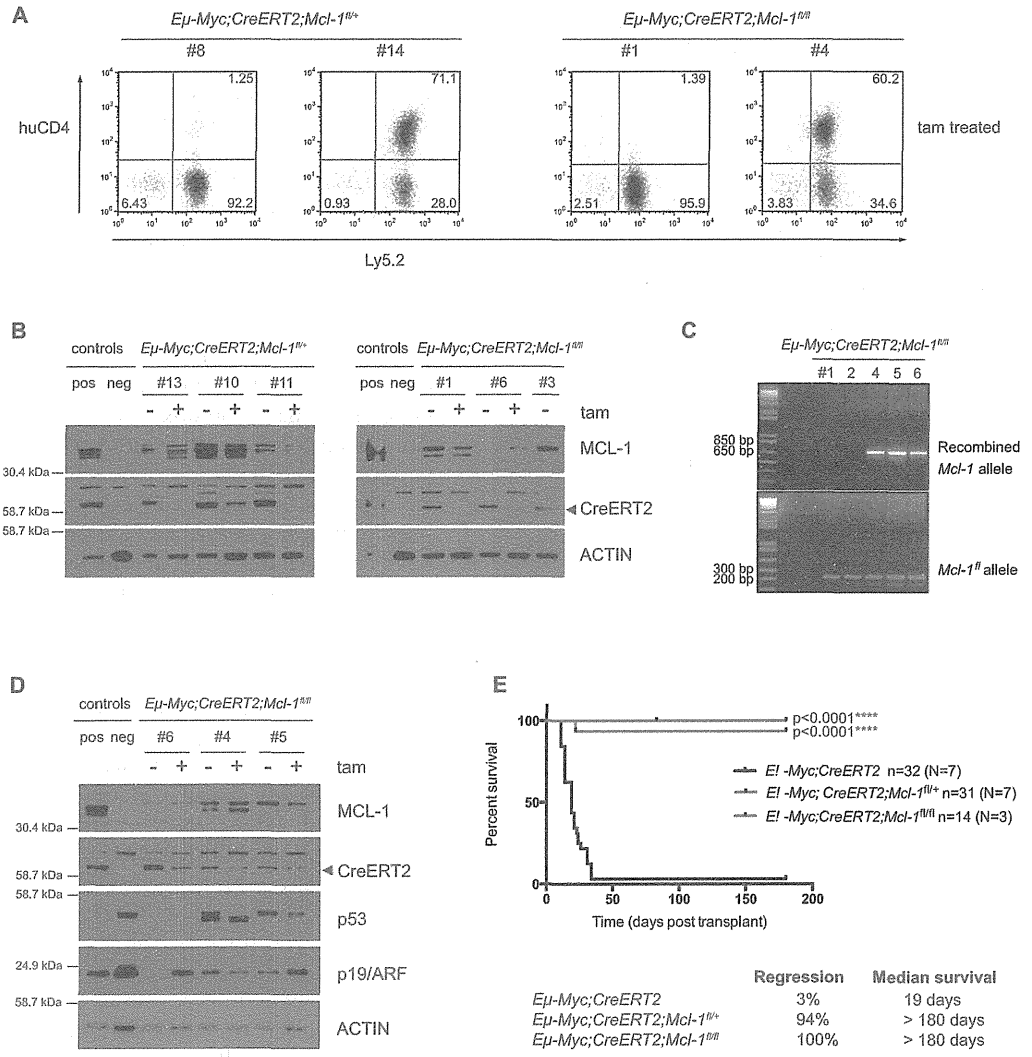

Figure 3. Most *Eμ-Myc* lymphomas that relapse following tamoxifen treatment have escaped *Mcl-1*^{fl} allele recombination. (*A*) FACS analysis to detect expression of huCD4 (reporter for *Mcl-1*^{fl} recombination) on the surface of two representative *Eμ-Myc;CreERT2;Mcl-1*$^{fl/+}$ and *Eμ-Myc;CreERT2;Mcl-1*$^{fl/fl}$ lymphomas that had relapsed in recipient mice after tamoxifen treatment (transplanted lymphoma cells stained positive for Ly5.2). Approximately 60% of the relapsed *Eμ-Myc;CreERT2;Mcl-1*$^{fl/+}$ and 40% of the relapsed *Eμ-Myc;*CreERT2;*Mcl-1*$^{fl/f}$ lymphoma cells had escaped *Mcl-1*^{fl} allele recombination and, as such, were huCD4-negative (like the sample at the *left* of each pair), whereas ~40% of the relapsed *Eμ-Myc;*CreERT2;*Mcl-1*$^{fl/+}$ and 60% of the relapsed *Eμ-Myc;CreERT2;Mcl-1*$^{fl/fl}$ lymphomas had efficiently recombined at least one *Mcl-1*^{fl} allele, as reflected by staining positive for huCD4 (like the sample at the *right* of each pair). (*B*) Immunoblotting to detect MCL-1 and CreERT2 protein expression (probing for Actin was used as a loading control) in extracts from the spleens, lymph nodes, or thymuses of sick mice that had been transplanted with *Eμ-Myc;CreERT2;Mcl-1*$^{fl/+}$ or *Eμ-Myc;*CreERT2;*Mcl-1*$^{fl/fl}$ lymphomas. Three independent, paired control, and tamoxifen-treated tumors of each genotype were analyzed (note that one of the *Eμ-Myc;CreERT2;Mcl-1*$^{fl/fl}$ tumors [#3] examined never relapsed after tamoxifen treatment). *Mcl-*1 knockout (KO) mouse embryonic fibroblasts (MEFs) were used as a control to confirm the specificity of the MCL-1 antibody (neg control). (*C*) DNA PCR analysis of recombined *Mcl-1*^{fl} and unrecombined (intact) floxed alleles in *Eμ-Myc;CreERT2;Mcl-1*$^{fl/fl}$ lymphomas that relapsed following tamoxifen treatment. (*D*) Immunoblotting to detect MCL-1, CreERT2, p53, p19/ARF and Actin (loading control) protein expression in extracts from the spleens, lymph nodes, or thymuses of sick mice transplanted with *Eμ-Myc;CreERT2;Mcl-1*$^{fl/fl}$ lymphomas that relapsed as huCD4-positive following tamoxifen treatment. Three independent, paired control, and tamoxifen-treated tumors were analyzed. *Mcl-1* knockout (KO) MEFs were used as a control (neg control) to confirm the specificity of the MCL-1 antibody. (*E*) Survival curves of C57BL/6-Ly5.1^{+} recipient mice transplanted with *Eμ-Myc;CreERT2;Mcl-1*$^{fl/+}$ (red line) or *Eμ-Myc;CreERT2;Mcl-1*$^{fl/fl}$ (blue line) lymphoma cells that had wild-type *p53* genes following tamoxifen treatment and excluding those lymphomas that escaped Cre-mediated deletion of one or both *Mcl-1*^{fl} alleles. C57BL/6-Ly5.1^{+} recipient mice transplanted with control (*Eμ-Myc;CreERT2*; black line) lymphoma cells and treated with tamoxifen are shown for comparison. (n) Total number of recipient mice analyzed; (N) number of independent lymphomas tested. Efficient heterozygous and homozygous deletion of *Mcl-1* significantly delayed lymphoma growth. (****) $P < 0.0001$. For the mice transplanted with the control *Eμ-Myc;CreERT2* lymphomas, 3% regressed, and the overall median survival was 19 d. For the mice transplanted with the *Eμ-Myc;CreERT2;Mcl-1*$^{fl/+}$ lymphomas, 94% regressed, and the overall median survival was >180 d. For the mice transplanted with the *Eμ-Myc;CreERT2;Mcl-1*$^{fl/fl}$ lymphomas, 100% regressed, and the overall median survival was >180 d.

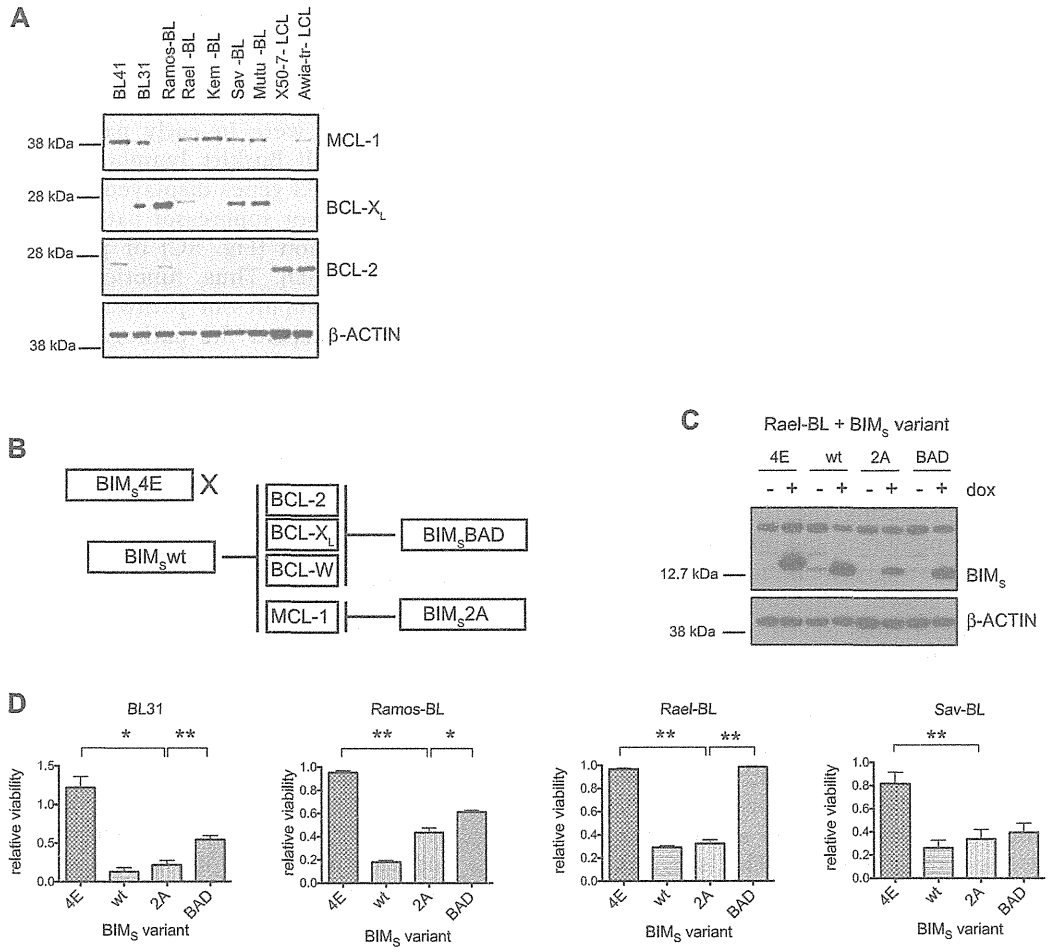

Figure 4. MCL-1 blockade kills human Burkitt lymphoma cells, but some also show minor dependency on BCL-X_L. (*A*) Immunoblotting to detect MCL-1, BCL-X_L, BCL-2, and β-Actin (loading control) in extracts from Burkitt lymphoma cell lines and, as controls for BCL-2 expression, the X50-7 and Awia lymphoblastoid cell lines. (*B*) Schematic showing the binding specificities of the BIM_S variants to the BCL-2 prosurvival proteins. (*C*) Immunoblotting to detect the inducible expression of the BIM_S variants before and after 24 h of dox treatment in the Rael-BL cell lines carrying the different lentiviral-inducible BIM_S expression constructs. Cells were maintained in medium supplemented with the pan-caspase inhibitor qVD-OPh to prevent protein degradation due to apoptosis. Note that the endogenous BIM_{EL}, BIM_L, and BIM_S proteins can also be detected but at a lower level. Probing for β-Actin served as a loading control. (*D*) Viability of BL cell lines stably infected with lentiviral constructs carrying vectors for dox-inducible expression of BIM_S variants was determined 72 h after the addition of dox to the medium by staining the cells with propidium iodide (PI) followed by FACS analysis for PI and GFP fluorescence (GFP is expressed from the lentivirus encoding the BIM_S variants). The PI-negative/GFP-positive viable cells were recorded. The percentage of viable/GFP-positive untreated cells was assigned an arbitrary value of 1, and the percentage of viable/GFP-positive dox-treated cells was expressed as a proportion of this. Each line was assayed in triplicate, and data are presented as the mean and standard error of the mean of three independent experiments. Statistical analysis using a paired two-tailed *t*-test showed that BIMs2A induced significantly more death in all of the Burkitt lymphoma cells examined compared with the negative control BIMs4E (BL31, [*] $P = 0.0179$; Ramos-BL, [**] $P = 0.0025$; Rael-BL, [**] $P = 0.0017$; Sav-BL, [**] $P = 0.0044$) and that BIMs2A induced significantly more death than BIMsBAD in BL31 ([**] $P = 0.0056$), Ramos-BL ([*] $P = 0.0421$), and Rael-BL ([**] $P = 0.0023$) cells but not in the Sav-BL cells ([ns] $P = 0.1348$). See also Supplemental Figure 4.

Notably, all Burkitt lymphoma cells were sensitive to BIM_S2A, indicating a dependency on MCL-1 (Fig. 4D; Supplemental Fig. 4D). Ramos-BL, BL31, and Sav-BL were also sensitive to BIM_SBAD (and, accordingly, also to treatment with ABT-737, which targets BCL-X_L, BCL-2, and BCL-W), albeit for Ramos-BL and BL31, significantly less than to BIM_S2A, indicating only a partial dependency on BCL-X_L (Fig. 4D; Supplemental Fig. 4C,D). Kinetic binding analyses using the Biacore confirmed that the more potent killing activity of BIM_S2A versus BIM_SBAD on most cell lines reflected the dependence of these cells on MCL-1 rather than a greater capacity of BIM_S2A to engage MCL-1 compared with the ability of BIM_SBAD to bind BCL-X_L. Indeed these Biacore binding assays showed that the affinity of the BAD-BH3 is actually ~20-fold higher for BCL-X_L (similar to that of wild-type BIM_S BH3) than the affinity of BIM_S2A for MCL-1 due to a significantly faster dissociation rate in the MCL-1 interaction

(Supplemental Fig. 4E). Collectively, these results show that the sustained survival and growth of Burkitt lymphoma cells is dependent on MCL-1 either alone or with a contribution by BCL-X_L.

Mutations in p53 reduce but do not ablate the dependency of c-MYC-driven mouse and human lymphomas on MCL-1

Although most transplanted *Eμ-Myc* mouse lymphomas (14 from 23 analyzed) could not continue to grow following heterozygous recombination of *Mcl-1^{fl}*, a minority of relapsing lymphomas (nine from 23 analyzed) did display heterozygous *Mcl-1^{fl}* allele deletion, as demonstrated by huCD4 immunostaining (Fig. 3A). We were interested to understand why these lymphoma cells were less dependent on MCL-1 for their growth, since such insights will be critical for predicting the therapeutic response of c-MYC-driven lymphomas and other cancers to MCL-1 antagonists. Interestingly, we noticed that most lymphomas capable of growth following transplantation and heterozygous *Mcl-1^{fl}* loss (seven of nine identified) displayed dramatically increased expression of the tumor suppressor p53 (Figs. 3D, 5A), a hallmark of *p53* gene mutations. DNA sequence analysis confirmed the presence of mutations affecting known "hot spot" residues (Freed-Pastor and Prives 2012) within the DNA-binding domain of p53 in the primary lymphomas capable of growth following transplantation and heterozygous deletion of *Mcl-1* (Figs. 3D, 5B). This suggests that the presence of existing mutations in the *p53* gene decreased the dependency of these tumor cells on MCL-1. An additional relapsed lymphoma of genotype *Eμ-Myc; CreERT2;Mcl-1$^{fl/fl}$* (#6) showed evidence of p53 pathway mutation (increased p19/ARF protein expression) upon tamoxifen treatment (increasing the frequency to eight of nine lymphomas showing perturbation of the p53 pathway) (Fig. 3D). As a control, we sequenced the p53 gene in seven of the 14 lymphomas that expressed physiological (i.e., very low/barely detectable in the absence of genotoxic stress) levels of p53 (indicative of wild-type nonmutated *p53* genes) and were not capable of growing following heterozygous loss of *Mcl-1* and confirmed that their *p53* genes were wild type. This highlights a novel and highly specific interplay between malignant cell survival dependency on MCL-1 and the p53 tumor suppressor pathway. Importantly, a lymphoma of genotype *Eμ-Myc;CreERT2;Mcl-1$^{fl/fl}$* (#3) carrying the *p53* mutation that introduced a stop codon almost always regressed following tamoxifen treatment. These results suggest that mutations in the p53 pathway and complete loss of wild-type p53 were not sufficient to allow sustained expansion of *Eμ-Myc* lymphomas with homozygous *Mcl-1* loss.

Therefore, and since mutations in *p53* are a common feature of many human cancers (Vousden and Lane 2007), we investigated whether p53 pathway defects could render Burkitt lymphoma cells resistant to MCL-1 targeting. Mutations of the *p53* gene, clustering around "hot spot" residues in the DNA-binding domain that are known to abrogate p53 function (Cho et al. 1994; Petitjean et al. 2007; Freed-Pastor and Prives 2012), were detected in Rael-BL, Sav-BL, and BL-31 and globally in ~60% of the 16 Burkitt lymphoma cell lines tested (note that many lines were in early passage) (Fig. 5C,D). Importantly, all Burkitt lymphoma cells that retained wild-type *p53* genes displayed other abnormalities in the p53 tumor suppressor pathway, including HDM2 overexpression (Fig. 5C) or p14ARF locus deletion (BL2) (Fig. 5D). Thus, functional inactivation of the p53 tumor suppressor pathway appears to constitute a critical step in the pathogenesis of c-MYC-driven Burkitt lymphoma but is insufficient to overcome the exquisite growth dependency of these malignant cells on MCL-1. Therefore, therapeutic targeting of MCL-1 would still remain an effective treatment regime for Burkitt lymphoma and possibly other c-MYC-driven human cancers.

Discussion

Up to 70% of human cancers display deregulated c-MYC overexpression (Boxer and Dang 2001; Sanchez-Beato et al. 2003). Identifying the cellular factors critical for the growth of c-MYC-driven cancers therefore remains an important objective for designing novel treatment strategies.

We investigated this by using two novel, innovative approaches: conditional deletion of *Mcl-1* or *Bcl-x* genes at will in *Eμ-Myc* lymphomas within the whole mouse or inducible expression of polypeptides that inhibit specific BCL-2 prosurvival proteins (mimicking the action of drugs that target these proteins; e.g., ABT-737 or ABT-263/navitoclax) in human Burkitt lymphoma cells. We found that although BCL-X_L is essential for *Eμ-Myc*-induced lymphoma development (Kelly et al. 2011), the loss of BCL-X_L had only a minimal impact on sustained tumor growth. Consistent with this, treatment of *Eμ-Myc* lymphomas with the BH3 mimetic ABT-737, which targets BCL-2, BCL-X_L, and BCL-W (Oltersdorf et al. 2005; van Delft et al. 2006), does not cause tumor regression (Mason et al. 2008), suggesting that these three prosurvival proteins are dispensable for sustained *Eμ-Myc* lymphoma growth. In contrast, sustained growth of *Eμ-Myc* lymphomas was exquisitely dependent on MCL-1. Remarkably, even heterozygous deletion of *Mcl-1* was sufficient to result in complete regression of ~20% of tumors, allowing long-term survival of formerly lymphoma-burdened mice. Strikingly, analysis of the lymphomas that did relapse revealed that ~60% had escaped *Mcl-1* deletion (mostly due to loss of the Cre recombinase). Indeed, when the animals bearing lymphomas that escaped *Mcl-1^{fl}* allele deletion (and had not acquired mutations in p53) were removed from the analysis, nearly 100% survived lymphoma-free long-term (>180 d post-transplant) (Fig. 3E). Importantly, this translated into the human disease setting, where we found that MCL-1 blockade efficiently killed Burkitt lymphoma cells, with a lesser impact of BCL-X_L targeting observed in some lines.

An MCL-1 dependency was also detected in AML mouse models and human AML-derived cell lines (Xiang

A

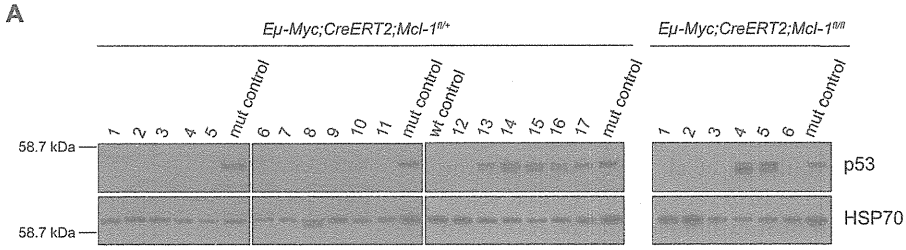

B

Mouse genotype	Mouse *p53* mutation	Homozygous/ heterozygous mutation	Frequency (No. of tumors)	Equivalent affected human *p53* aa
Eμ-Myc;CreERT2;Mcl-1$^{fl/+}$	V170M	hom	1	V173
	I192S	het	1	I195
	R246Q	hom	1	R249
	R270H	hom	1	R273
	280G insertion	hom	1	R283
Eμ-Myc;CreERT2;Mcl-1$^{fl/fl}$	R270H	hom	2	R273
	S224 (deletion of 2bps)	hom	1	S227

C

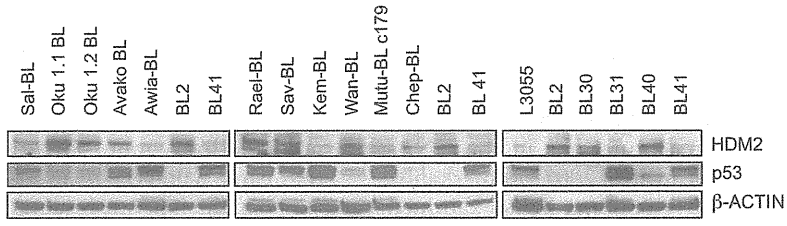

D

BL cell line	p53 gene mutation	HDM2 expression	$p14^{ARF}$ locus
Sal-BL	WT	Mid	Intact
Oku-BL	WT	High	Intact
Wan-BL	WT	High	Intact
Chep-BL	WT	Mid	Intact
BL2	WT	High	Deleted
BL30	WT	High	Intact
BL40	WT	High	Intact
Rael-BL	R282W	High	Intact
Kem-BL		Low	Intact
L3055		Low	Intact
BL31	V172F	Low	Intact
Sav-BL	G244D	High	Intact
Mutu-BL cl 179	G245D	Low	Intact
Ava-BL	M246T	Mid	Intact
BL41	R248Q	Low	Intact
Awia-BL	Deletion of Q165, S166, Q167	Low	Intact

Figure 5. Mutations in *p53* reduce but do not ablate the dependency of c-MYC-driven mouse and human lymphomas on MCL-1. (*A*) Immunoblotting to detect stabilized p53 proteins, indicative of a mutant p53 protein, in extracts from 17 *Eμ-Myc;CreERT2;Mcl-1*$^{fl/+}$ and six *Eμ-Myc;CreERT2;Mcl-1*$^{fl/fl}$ lymphomas. All but two of the samples were extracted from transplanted and tamoxifen-treated lymphomas. The two exceptions were *Eμ-Myc;CreERT2;Mcl-1*$^{fl/+}$ #9, which was a primary lymphoma, and *Eμ-Myc;CreERT2;Mcl-1*$^{fl/fl}$ #3, which was a transplanted but not tamoxifen-treated lymphoma (this particular lymphoma has the deletion of two bases that introduces a premature stop codon in the *p53* gene). Probing for HSP70 served as a loading control. (*B*) Summary of the *p53* mutations detected in *Eμ-Myc;CreERT2;Mcl-1*$^{fl/+}$ and *Eμ-Myc;CreERT2;Mcl-1*$^{fl/fl}$ lymphomas as detected by DNA sequence analysis. The mutations are listed as wild-type (wt) amino acid (aa) affected, amino acid position, and mutant amino acid. The frequencies at which the mutations were detected in the lymphomas and the human equivalents of the mutations are listed. The sequence alignment for murine *p53* was performed using Ensembl transcript number ENSMUST00000108658 as the reference transcript. (*C*) Immunoblotting to detect the expression of HDM2, p53, and β-Actin (loading control) in human Burkitt lymphoma cell lines. (*D*) Summary of the *p53* pathway aberrations detected in the human Burkitt lymphoma cell lines. The *p53* mutations present in each cell line is listed as wild-type (wt) amino acid (aa) affected, amino acid position, and mutant amino acid, and the number of alleles affected is also detailed.

et al. 2010; Glaser et al. 2012). This finding and the observation that ~10% of diverse tumors contain somatically acquired amplifications of the genomic region harboring *MCL-1* (Beroukhim et al. 2010) highlight the importance of developing BH3 mimetic drugs that selectively target MCL-1 for treating human cancers. A concern is that MCL-1 is required for the survival of hematopoietic stem/progenitor cells (Opferman et al. 2005) and several other critical cell types, including cardiomyocytes (Opferman et al. 2003; Vikstrom et al. 2010; Thomas et al. 2013; Wang et al. 2013). Importantly, our discovery that MYC-driven lymphomas cannot tolerate even heterozygous loss of *Mcl-1* (which should mimic 50% drug-mediated inhibition of the protein), whereas its heterozygous loss is well tolerated in normal tissues (Opferman et al. 2003, 2005; Vikstrom et al. 2010), indicates that it should be possible to establish a therapeutic window for MCL-1 inhibitory drugs.

A novel and highly important finding from this study is the observation that mutations in "hot spot" residues in the DNA-binding domain of the *p53* gene can reduce but not abrogate the lymphoma cells' dependency on MCL-1. Consistent with a recent study that found that *p53* mutations are the fourth most commonly detected genetic change in a large panel of Burkitt lymphoma biopsies (Love et al. 2012), we found that ~60% of Burkitt lymphoma lines had acquired mutations in the DNA-binding domain of *p53* (Petitjean et al. 2007). Remarkably, all of the remaining Burkitt lymphoma lines examined displayed some other abnormalities in components of the p53 pathway, such as HDM2 overexpression or p14/ARF loss. Importantly, MCL-1 antagonism was able to kill Burkitt lymphomas with p53 pathway defects, suggesting that MCL-1 inhibitory drugs could be efficacious in the treatment of c-MYC-driven cancers bearing *p53* mutations.

The network of processes that p53 activates to suppress tumorigenesis are still emerging (Brady et al. 2011; Li et al. 2012; Valente et al. 2013). The observation that mutation and loss of *p53* constitute critical steps in c-MYC-driven lymphomagenesis (Vousden and Lane 2007; Michalak et al. 2009) and that they can facilitate the sustained growth of malignant *Eμ-Myc* lymphomas with reduced MCL-1 expression highlights the connection between the p53 tumor suppressor pathway and the dependency of malignant cells on prosurvival MCL-1.

Our results are consistent with a model (Fig. 6) in which c-MYC-driven lymphomas are highly dependent on MCL-1 for survival. A reduction of MCL-1 expression through either genetic means or, in the future, therapeutics could induce cell death by disturbing the balance between the proapoptotic p53 targets PUMA/NOXA and prosurvival MCL-1. However, when designing therapeutic strategies for such lymphomas, we need to be mindful that mutations in *p53* would prevent oncogenic stress-induced up-regulation of PUMA and NOXA and may thereby render lymphoma cells less dependent on MCL-1. Therefore, for such (*p53* mutated) c-MYC-driven lymphomas, it may be beneficial to activate the intrinsic apoptotic pathway more potently than is needed for tumors that carry wild-type *p53*.

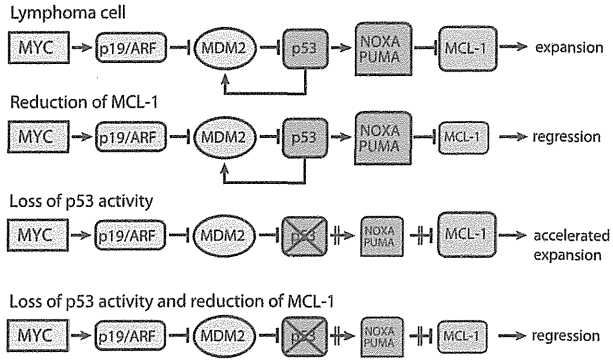

Figure 6. A proposed model in which c-MYC-driven lymphoma cells that are highly dependent on MCL-1 for their sustained expansion can no longer survive once MCL-1 expression is reduced and the balance between this prosurvival protein and the *p53* proapoptotic targets PUMA/NOXA is disturbed. The c-MYC-driven lymphoma cells that have acquired *p53* mutations display an accelerated lymphoma progression. These lymphomas express less PUMA/NOXA, and, consequently, less MCL-1 expression is required to maintain the lymphoma progression. Despite this, we showed that targeting of MCL-1 in lymphomas with *p53* mutations was sufficient to result in tumor regression. Note that the mouse protein nomenclature is used.

In conclusion, our findings suggest that MCL-1 targeting may be a viable strategy for cancer therapy, particularly in tumors where deregulated c-MYC expression instills an exquisite dependence (much more so than in nontransformed cells) on this prosurvival protein.

Materials and methods

Mice

Experiments with mice were conducted according to the guidelines of The Walter and Eliza Hall Institute Animal Ethics Committee. *Eμ-Myc* transgenic (Adams et al. 1985), *Bcl-x*$^{fl/fl}$ (Wagner et al. 2000), *Mcl-1*$^{fl/fl}$ (Vikstrom et al. 2010), *Rosa26-CreERT2* (Seibler et al. 2003), and *p53*$^{-/-}$ (Jacks et al. 1994) gene targeted mice have all been described previously. All mouse strains were on a C57BL/6-Ly5.2^{+} genetic background generated on either this background (*Mcl-1*$^{fl/fl}$ and *Rosa26-CreERT2*) using C57BL/6-derived embryonic stem cells, a mixed C57BL/6x129SV background (*Bcl-x*$^{fl/fl}$) using 129SV-derived embryonic stem cells, or a mixed C57BL/6xSJL background (*Eμ-Myc*) using microinjection of C57BL/6xSJL-derived oocytes and then backcrossed for 10 to >20 generations with C57BL/6 mice.

Single-cell suspensions of 3 × 10^{6} *Eμ-Myc* lymphoma cells in PBS were injected into C57BL/6-Ly5.1^{+} or C57BL/6J-Tyr$^{c\text{-}2J}$ (referred to as C57BL/6-albino; The Jackson Laboratory) recipient mice by intravenous (i.v.) tail vein injection. Mice were administered by oral gavage with 200 mg/kg tamoxifen (Sigma-Aldrich) in peanut oil/10% ethanol per day (Anastassiadis et al. 2010) for two consecutive days on either days 5 and 6 or days 10 and 11 post-injection of the tumor cells. Transplants in which the matched control untreated mice did not become sick by 28 d post-tumor cell injection were excluded from the analysis.

Statistical analysis

Graphpad Prism software was used for generating Kaplan-Meier plots and performing statistical analysis (using a log-rank test) to compare the survival of mice injected with lymphoma cells of different genotypes. Graphpad Prism was also used to carry out paired two-tailed *t*-tests on the death induced in the Burkitt lymphoma cells following dox-inducible expression of the BIMs variants. Specifically, the significance of the extent of cell death induced by BIMs2A (to target MCL-1) expression compared with either inducible expression of BIMs4E (negative control) or BIMsBAD (to target BCL-2, BCL-X_L, and BCL-W) was calculated for each of the Burkitt lymphoma cell lines.

Cell culture

Eμ-Myc mouse lymphoma cells were cultured in high-glucose Dulbecco's modified Eagle's medium (DMEM) supplemented with 10% fetal bovine serum (FBS) (Gibco), 50 μM β-mercaptoethanol (Sigma-Aldrich), 100 μM asparagine (Sigma-Aldrich), 100 U/mL penicillin, and 100 mg/mL streptomycin (Gibco) at 37°C and 10% CO_2. OP9 cells were cultured in αMEM (Gibco) supplemented with 20% heat-inactivated FBS, 1 mM glutamine (Gibco), 10 mM Hepes (Gibco), 1 mM sodium pyruvate (Gibco), 50 μM β-mercaptoethanol, 100 U/mL penicillin, and 100 μg/mL streptomycin. Human cell lines were cultured in a humidified incubator at 37°C and 5% CO_2. Virus-producing 293T cells were maintained in DMEM supplemented with 10% FBS. Approximately 6 h prior to transfection, 293T cells were cultured in DME glutamax (Gibco) supplemented with 10% FBS and 25 mM Hepes. Rael-BL, Ramos-BL, Sav-BL, and BL-31 human Burkitt lymphoma-derived cell lines were cultured in RPMI 1640 supplemented with 10% FBS, 1 mM glutamine (Gibco), 1 mM sodium pyruvate (Gibco), 50 μM α-thioglycerol (Sigma-Aldrich), and 20 nM bathocuproine disulfonic acid (BCS) (Sigma-Aldrich). X50-7 and Awia lymphoblastoid cell lines were cultured in RPMI 1640 supplemented with 10% FBS and 1 mM glutamine.

Lentiviral plasmids and virus production

The dox-responsive lentiviral vector pFTRE3G_pGK3G_GFP was generated by digesting PacI/AscI and cloning the TRE3G_pGK3G_GFP cassette. The TRE3G_pGK3G GFP cassette was amplified by PCR as pTRE3G_pGK3G_GFP (Yamamoto et al. 2012). The PCR products of the BIM_S variants (Lee et al. 2008) were cloned into pFTRE3G_pGK3G_GFP. The lentiviral imaging construct was generated by inserting Luciferase2 linked via a T2A peptide to eGFP downstream from the human ubiquitin promoter of the FUGW vector (Lois et al. 2002). Lentivirus-containing supernatants were produced by transiently transfecting 293T cells with the expression constructs of interest alongside the packaging plasmids, VSV-G, MDL, and RSV-Rev using the standard $CaPO_4$ method (Herold et al. 2008). Supernatants containing infectious virus particles were harvested 2–3 d post-transfection.

Lentiviral transduction of Eμ-Myc lymphoma cells and Burkitt lymphoma cell lines

For infection, aliquots of 0.5×10^6 to 1×10^6 primary *Eμ-Myc* lymphoma cells or 1×10^5 Burkitt lymphoma cells were suspended in 4 mL of virus-containing supernatant containing 10 ng/μL polybrene, incubated for 30 min at 37°C and 5% or 10% CO_2, and then centrifuged at 2200 rpm for 2.5 h at 32°C. The supernatant was subsequently discarded, and the cells were resuspended in fresh medium for culture.

Inducible expression of BIM_S variants in human Burkitt lymphoma cells

To induce expression of the BIM_S variants, cells were cultured in medium supplemented with 1 μg/mL dox. The viability of the GFP-positive cells was determined by propidium iodide (PI) staining and FACS analysis in an LSR1 machine. The PI-negative/GFP-positive cells were considered as live cells. The cell death following inducible expression of the BIMs variant was expressed relative to the untreated Burkitt lymphoma cells, which were assigned a value of 1. For the analysis of the BIM_S variant expression by immunoblotting, the pan-caspase inhibitor qVD-OPh (25 μM; MP Biomedicals) was added to the dox-treated cells for 24 h to inhibit cell killing.

Direct binding assays to determine the binding parameters of BH3 ligands for BCL-X_L and MCL-1

Direct binding assays were performed at room temperature using a Biacore S51 biosensor exactly as described previously (Lee et al. 2007). The peptides used were BIMs BH3, DMRPEIWIAQELRR IGDEFNAYYARR; BIM_S 2A BH3, DMRPEIWIAQEARRIGDEA NAYYARR; and BAD_S BH3, NLWAAQRYGRELRRMSDEFVD SFKKG.

Immunofluorescent staining, flow cytometric analysis, and cell sorting

To immunophenotype *Eμ-Myc* lymphomas, single-cell suspensions were stained as described (Strasser et al. 1991) with surface marker-specific antibodies and analyzed using an LSR1 machine (Becton Dickinson). The following fluorochrome-conjugated antibodies were used: CD19 (clone ID3), B220 (RA3-6B2), IgM (clone 5.1), IgD (clone 11-26C), CD4 (clone H129), CD8 (clone YTS.169), Thy1 (clone T3.24.1), Mac1 (M1/70), and GR1 (clone RB6-8C5). To discriminate host-derived ($Ly5.1^+$) from donor-derived ($Ly5.2^+$) cells, monoclonal antibodies to Ly5.1 (clone A201.1) and Ly5.2 (clone 5.450.15.2 or AL14A7) were used. To verify recombination of the *loxP*-flanked allele of *Mcl-1*, cells were stained with antibodies to human CD4 (clone RPA-T4), since $Mcl\text{-}1^{fl}$ recombination subjugates a human CD4 reporter cassette to the *Mcl-1* promoter/enhancer (Vikstrom et al. 2010). Antibodies were produced in our laboratory and conjugated to FITC, R-phycoerythrin (R-PE), or allophycocyanin (APC) according to the manufacturers' instructions. Where required, Burkitt lymphoma cells were sorted for GFP expression using an AriaW cell sorter (Becton Dickinson).

Immunoblotting

Total protein extracts were prepared from cells (primary *Eμ-Myc* lymphomas and Burkitt lymphoma cell lines) by lysis in onyx buffer, NP40 buffer, or urea buffer containing protease inhibitors (Complete protease inhibitor cocktail, Roche). Protein content was quantified using the Bio-Rad Bradford assay. Total protein extracts (20 μg) were separated on the basis of molecular weight by SDS-PAGE and Western-blotted onto nitrocellulose membranes. The membranes were blocked in 5% skim milk in PBS and 0.1% Tween20 (blocking buffer) before incubation with antibodies. Polyclonal antibodies were used to detect mouse MCL-1 (Rockland Antibodies and Assays), BIM (Enzo Life Sciences), BCL-x (BD Biosciences), and human MCL-1 (s-19, Santa Cruz Biotechnology); monoclonal antibodies were used to detect mouse p53 (clone IMX25, Novocastra), p19/ARF (clone 5.C3.1, Rockland Antibodies and Assays), ERα (to detect the CreERT2 protein) (clone HC-20, Santa Cruz Biotechnology),

Actin (clone AC40, Sigma-Aldrich), and β-Actin (clone AC74, Sigma-Aldrich); and monoclonal antibodies were used to detect human p53 (clone FL393), HDM2 (clone N20), BCL-2 (clone C-2), BCL-X_L (clone H5) (all from Santa Cruz Biotechnology), β-Actin (clone AC15, Sigma-Aldrich), and HSP70 (mouse monoclonal antibody clone N6; detects both mouse and human protein) (a gift from Dr R Anderson, Peter MacCallum Cancer Research Institute, Melbourne, Australia). All antibodies were diluted in blocking buffer.

qRT–PCR analysis

Total RNA was extracted from paired untreated and tamoxifen-treated *Eμ-Myc* lymphoma cells using TRIzol reagent (Invitrogen) according to the manufacturer's instructions. The RNA was treated with DNase to remove contaminating DNA using the RNase-free DNase Qiagen kit according to the manufacturer's instructions. RNA quality and quantity were determined using the NanoDrop assay (Thermo Fisher Scientific). Aliquots of 1 μg of RNA were reverse-transcribed into cDNA using the SuperScript III first strand synthesis Supermix kit (Invitrogen) in a 20-μL reaction volume according to the manufacturer's instructions. The cDNA was diluted 10-fold in H_2O, and PCR amplifications of 1 μL of cDNA were performed with an Applied Biosystems 7900HT thermal cycler using TaqMan Universal PCR Mastermix and 0.5 μL of TaqMan primer/probes (both Applied Biosystems) in a 10-μL reaction volume. Assays specific for *Bcl-x* (Mm00437783) and (as an endogenous control for RNA quality/input) HMBS (Mm01143545) transcripts were performed. Three replicates of each reaction were performed. All qPCR data were analyzed using the $2^{-\Delta\Delta CT}$ method and expressed relative to the untreated sample of each pair.

IVIS imaging

Single-cell suspensions of lymphoma cells taken from the lymph nodes, spleens, or thymuses of sick *Eμ-Myc;CreERT2,Bcl-x$^{fl/fl}$* and *Eμ-Myc;CreERT2;Mcl-1$^{fl/fl}$* mice were transduced with a GFP-luc lentiviral vector as described above. Transduced cells were cultured for three passages on an OP9 cell feeder layer (Zúñiga-Pflücker et al. 1994) and then washed in PBS, and 4×10^5 to 1×10^6 live lymphoma cells were injected i.v. into C57BL/6-albino recipient mice. To visualize the tumor burden, 200 μL of 15 mg/mL D-luciferin potassium salt (Caliper Life Sciences) in PBS was administered to the mice by intraperitoneal (i.p.) injection. Mice were then anaesthetized with isoflurane inhalant and imaged using the IVIS live-imaging system (Perkin Elmer) to detect luciferase bioluminescence exactly 15 min after administration of the luciferin substrate. The tumor burden was quantified by measuring the total photon flux per second emitted from a region of interest (ROI) drawn around the whole mouse. When the lymphoma burden was sufficiently high (photon flux per second of $>1 \times 10^7$), some mice from each cohort were administered tamoxifen by oral gavage once per day for three consecutive days, and the tumor regression/progression was monitored by further bioluminescence imaging at indicated time points.

Human p53 cDNA sequence analysis

The human *p53* gene status was determined by sequencing of cDNA (Lindstrom et al. 2001). Total RNA was extracted from cells using TRIzol reagent (Invitrogen) according to the manufacturer's instructions. The cDNA was made from total RNA using the Advantage one-step RT–PCR kit according to the manufacturer's instructions (Clontech). *p53* was sequenced from pooled PCR reactions using the following primers: p53F1 (5′-GAAGGATCCGAGGAGCCGCAGT-3′), p53F781 (5′-CTGAGGTTGGCTCTGACTGTACCACCATCC-3′), p53R789 (5′-AACAAGCTTATTACCACTGGAGTCTTC-3′), and p53R1179 (5′-AGGGAATTCAGTCTGAGTCAGGC-3′).

DNA extraction, PCR, and DNA sequence analysis

DNA was extracted from cells using the Qiagen DNEasy tissue kit (Qiagen) according to the manufacturer's instructions, and the DNA concentration was quantified using the Nanodrop assay. Exons 4, 5–6, 7, 8–9, and 10 of the mouse *p53* gene were PCR-amplified from 100 ng of DNA using GoTaq green master mix (M712, Promega) and 3.3 μM primers using 32 cycles of 1 min at 94°C, 1 min at 52°C, and 1 min at 72°C followed by a 5-min extension at 72°C. DNA sequence analysis was performed by Micromon Monash. The following primer combinations were used to PCR-amplify and sequence mouse *p53*: Ex4F (5′-GGTTCTTCTTTGTCCCATCC-3′) with Ex4R (5′-GAGGCATTGAAAGGTCACAC-3′), Ex5F 5′-TTAGTTCCCCACCTTGACAC-3′) with Ex6R (5′-AGGCTGGAGTCAACTGTCTC-3′), Ex7F (5′-TAGTGAGGTAGGGAGCGACTTC-3′) with Ex7R (5′-CCAAGAGGAAACAGAGGAGG-3′), Ex8F (5′-CTTCTCGGGGTTCCTGTAAC-3′) with Ex9R (5′-CCTGGCAACCTGCTAATAAC-3′), and Ex10F (5′-AAACCTGTAAGTGGAGCCAG-3′) with Ex10R (5′-AGTCAGTTCTCGTAGGGTGC-3′). The sequence alignment for murine *p53* was performed using Ensembl transcript number ENSMUST00000108658 as the reference transcript.

DNA PCR to detect Mcl-1^{fl}, Mcl-1^{wt}, and recombined Mcl-1 alleles

The wild-type, *Mcl-1^{fl}*, and recombined *Mcl-1^{fl}* alleles were PCR-amplified from 100 ng of DNA using GoTaq green master mix (M712, Promega) and 0.5 μM primers using 30 cycles of 40 sec at 94°C, 30 sec at 55°C, and 1 min at 72°C followed by a 5-min extension at 72°C. The following primers were used to detect *Mcl-1^{fl}* and *Mcl-1^{wt}* alleles: 5′-GCACAATCCGTCCGCGAGCCAA-3′ and reverse 5′-GCCGCAGTACAGGTTCAAG-3′. The wild-type PCR product was smaller than the floxed PCR product. The following primers were used to detect recombined *Mcl-1^{fl}* alleles: 5′-CGACACAGATCAGCAGGCGTTC-3′ with 5′-GAGTCAGCGCGATCATTCAGCT-3′.

DNA PCR to detect homozygous deletion of the CDKN2A (INK4A/ARF) locus

The following PCR primers were used: exon 1β, (F, 5′-TGCAGTTAAGGGGGCAGGAG-3′; R, 5′-TTATCTCCTCCTCCTCCTAGCCTG-3′) and exon 2 (551R, 5′-TCTGAGCTTTGGAAGCTCT-3′; 42F, 5′-GGAAATTGGAAACTGGAAGC-3′). A GAPDH exon 8 fragment served as control for integrity of DNA.

Acknowledgments

We thank G. Siciliano and his team for help with animal husbandry, C. McLean for editorial assistance, Dr. J.M. Adams and Dr. S. Cory for advice and discussions, and Dr. Kelly Rogers for help with imaging of mice. This work is supported by a Kay Kendall Leukemia Fund Intermediate Fellowship (KKL331) and an EMBO short-term fellowship (both awarded to G.L.K.); the National Health and Medical Research Council, Australia (program grant 1016701 and fellowship 1020363 to A.S., project grant APP1049720 to M.J.H., project grant APP1041936 to W.D.F., and career development fellowship APP1024620 to E.F.L.); Cancer Research UK (program grant awarded to L.F., M. Rowe, and

A.B.R.); the Leukemia Foundation; the Leukemia and Lymphoma Society (specialized center of research 7001-13); and a German Research Council Fellowship (He 5740/1-1 awarded to M.J.H.). This work was made possible through Victorian State Government Operational Infrastructure Support and Australian Government National Health and Medical Research Council Independent Research Institutes Infrastructure Support Scheme.

References

Adams JM, Harris AW, Pinkert CA, Corcoran LM, Alexander WS, Cory S, Palmiter RD, Brinster RL. 1985. The c-*myc* oncogene driven by immunoglobulin enhancers induces lymphoid malignancy in transgenic mice. *Nature* **318:** 533–538.

Anastassiadis K, Glaser S, Kranz A, Berhardt K, Stewart AF. 2010. A practical summary of site-specific recombination, conditional mutagenesis, and tamoxifen induction of CreERT2. *Methods Enzymol* **477:** 109–123.

Beroukhim R, Mermel C, Porter D, Wei G, Raychaudhuri S, Donovan J, Barretina J, Boehm J, Dobson J, Urashima M, et al. 2010. The landscape of somatic copy-number alteration across human cancers. *Nature* **463:** 899–905.

Bhatia KG, Gutierrez MI, Huppi K, Siwarski D, Magrath IT. 1992. The pattern of *p53* mutations in Burkitt's lymphoma differs from that of solid tumors. *Cancer Res* **52:** 4273–4276.

Boxer LM, Dang CV. 2001. Translocations involving c-*myc* and c-*myc* function. *Oncogene* **20:** 5595–5610.

Brady CA, Jiang D, Mello SS, Johnson TM, Jarvis LA, Kozak MM, Broz DK, Basak S, Park EJ, McLaughlin ME, et al. 2011. Distinct p53 transcriptional programs dictate acute DNA-damage responses and tumor suppression. *Cell* **145:** 571–583.

Chen L, Willis SN, Wei A, Smith BJ, Fletcher JI, Hinds MG, Colman PM, Day CL, Adams JM, Huang DCS. 2005. Differential targeting of pro-survival Bcl-2 proteins by their BH3-only ligands allows complementary apoptotic function. *Mol Cell* **17:** 393–403.

Cho Y, Gorina S, Jeffrey PD, Pavletich NP. 1994. Crystal structure of a p53 tumor suppressor-DNA complex: Understanding tumorigenic mutations. *Science* **265:** 346–355.

Dang CV. 1999. c-Myc target genes involved in cell growth, apoptosis, and metabolism. *Mol Cell Biol* **19:** 1–11.

Egle A, Harris AW, Bouillet P, Cory S. 2004. Bim is a suppressor of Myc-induced mouse B cell leukemia. *Proc Natl Acad Sci* **101:** 6164–6169.

Farrell PJ, Allan GJ, Shanahan F, Vousden KH, Crook T. 1991. p53 is frequently mutated in Burkitt's lymphoma cell lines. *EMBO J* **10:** 2879–2887.

Freed-Pastor WA, Prives C. 2012. Mutant p53: One name, many proteins. *Genes Dev* **26:** 1268–1286.

Garrison SP, Jeffers JR, Yang C, Nilsson JA, Hall MA, Rehg JE, Yue W, Yu J, Zhang L, Onciu M, et al. 2008. Selection against PUMA gene expression in Myc-driven B-cell lymphomagenesis. *Mol Cell Biol* **28:** 5391–5402.

Giulino-Roth L, Wang K, MacDonald TY, Mathew S, Tam Y, Cronin MT, Palmer G, Lucena-Silva N, Pedrosa F, Pedrosa M, et al. 2012. Targeted genomic sequencing of pediatric Burkitt lymphoma identifies recurrent alterations in antiapoptotic and chromatin-remodeling genes. *Blood* **120:** 5181–5184.

Glaser S, Lee EF, Trounson E, Bouillet P, Wei A, Fairlie WD, Izon DJ, Zuber J, Rappaport AR, Herold MJ, et al. 2012. Anti-apoptotic Mcl-1 is essential for the development and sustained growth of acute myeloid leukemia. *Genes Dev* **26:** 120–125.

Hanahan D, Weinberg RA. 2011. Hallmarks of cancer: The next generation. *Cell* **144:** 646–674.

Hemann MT, Zilfou JT, Zhao Z, Burgess DJ, Hannon GJ, Lowe SW. 2004. Suppression of tumorigenesis by the p53 target PUMA. *Proc Natl Acad Sci* **101:** 9333–9338.

Henderson S, Rowe M, Gregory C, Croom Carter D, Wang F, Longnecker R, Kieff E, Rickinson A. 1991. Induction of *bcl-2* expression by Epstein-Barr virus latent membrane protein 1 protects infected B cells from programmed cell death. *Cell* **65:** 1107–1115.

Herold MJ, van den Brandt J, Seibler J, Reichardt HM. 2008. Inducible and reversible gene silencing by stable integration of an shRNA-encoding lentivirus in transgenic rats. *Proc Natl Acad Sci* **105:** 18507–18512.

Jacks T, Remington L, Williams BO, Schmitt EM, Halachmi S, Bronson RT, Weinberg RA. 1994. Tumor spectrum analysis in *p53*-mutant mice. *Curr Biol* **4:** 1–7.

Jeffers JR, Parganas E, Lee Y, Yang C, Wang J, Brennan J, MacLean KH, Han J, Chittenden T, Ihle JN, et al. 2003. Puma is an essential mediator of p53-dependent and -independent apoptotic pathways. *Cancer Cell* **4:** 321–328.

Kelly GL, Strasser A. 2011. The essential role of evasion from cell death in cancer. *Adv Cancer Res* **111:** 39–96.

Kelly PN, Grabow S, Delbridge ARD, Strasser A, Adams JM. 2011. Endogenous Bcl-xL is essential for Myc-driven lymphomagenesis in mice. *Blood* **118:** 6380–6386.

Khaw SL, Huang DC, Roberts AW. 2011. Overcoming blocks in apoptosis with BH3-mimetic therapy in haematological malignancies. *Pathology* **43:** 525–535.

Langdon WY, Harris AW, Cory S, Adams JM. 1986. The c-*myc* oncogene perturbs B lymphocyte development in Eμ-*myc* transgenic mice. *Cell* **47:** 11–18.

Lee EF, Czabotar PE, Smith BJ, Deshayes K, Zobel K, Colman PM, Fairlie WD. 2007. Crystal structure of ABT-737 complexed with Bcl-x(L): Implications for selectivity of antagonists of the Bcl-2 family. *Cell Death Differ* **14:** 1711–1713.

Lee EF, Czabotar PE, van Delft MF, Michalak E, Boyle M, Willis SN, Puthalakath H, Bouillet P, Colman PM, Huang DCS, et al. 2008. A novel BH3 ligand that selectively targets Mcl-1 reveals that apoptosis can proceed without Mcl-1 degradation. *J Cell Biol* **180:** 341–355.

Lessene G, Czabotar PE, Colman PM. 2008. BCL-2 family antagonists for cancer therapy. *Nat Rev Drug Discov* **7:** 989–1000.

Li T, Kon N, Jiang L, Tan M, Ludwig T, Zhao Y, Baer R, Gu W. 2012. Tumor suppression in the absence of p53-mediated cell-cycle arrest, apoptosis, and senescence. *Cell* **149:** 1269–1283.

Lindstrom MS, Klangby U, Wiman KG. 2001. p14ARF homozygous deletion or MDM2 overexpression in Burkitt lymphoma lines carrying wild type p53. *Oncogene* **20:** 2171–2177.

Llambi F, Moldoveanu T, Tait SW, Bouchier-Hayes L, Temirov J, McCormick LL, Dillon CP, Green DR. 2011. A unified model of mammalian BCL-2 protein family interactions at the mitochondria. *Mol Cell* **44:** 517–531.

Lois C, Hong EJ, Pease S, Brown EJ, Baltimore D. 2002. Germline transmission and tissue-specific expression of transgenes delivered by lentiviral vectors. *Science* **295:** 868–872.

Love C, Sun Z, Jima D, Li G, Zhang J, Miles R, Richards KL, Dunphy CH, Choi WW, Srivastava G, et al. 2012. The genetic landscape of mutations in Burkitt lymphoma. *Nat Genet* **44:** 1321–1325.

Mason KD, Vandenberg CJ, Scott CL, Wei AH, Cory S, Huang DC, Roberts AW. 2008. In vivo efficacy of the Bcl-2 antagonist ABT-737 against aggressive Myc-driven lymphomas. *Proc Natl Acad Sci* **105:** 17961–17966.

Merino D, Giam M, Hughes PD, Siggs OM, Heger K, O'Reilly LA, Adams JM, Strasser A, Lee EF, Fairlie WD, et al. 2009.